Sandusky (1976) shows that if we start with one gram of tobacco, then after pyrolysis about 400 mg of charred residue remains. This char includes 150 mg of inert material, which remains as ash upon combustion. That is, about 70% (600 mg) of the combustible portion (850 mg) of the tobacco evaporates and/or pyrolyses away, leaving about 250 mg of material which can burn completely. To avoid confusion, we will refer to that portion as "char," and the char plus ash (total = 400 mg) as "charred tobacco residue," or CTR, hereafter. We will not go into any more detail here regarding pyrolysis rates.

2. Stoichiometry

We now try to determine a sensible approximation to the stoichiometry of the reactions. This will be useful when the production of CO, H_2O, and CO_2 are modeled. The contents of the tobacco are quite complex, as shown in Sandusky (1976) and elsewhere. The reactions are complex as well. A simplified summary of the reactions is given at the bottom of page V in Sandusky. This is here simplified still further, by assuming that the dehydration and pyrolysis processes leading to char have exothermic as well as endothermic terms which cancel exactly.

When the char burns, the principal products are CO and CO_2, leaving about 150/400 = 37.5% ash, by weight. This residue is somewhat higher than the amount left by the tobacco analyzed by Baker (1975). Sandusky's data is used here, complemented where necessary by Baker's data. Char is assumed to consist of a mixture of carbon and of one other compound which will yield C/H/O ratios comparable to those given by Baker, and for which we know the heat of combustion, H_c. A model molecule is mucic acid, $C_6H_{10}O_8$. This has the molar heat of combustion H_c = 2021 kJ/g mol (Weast, 1976). Its molecular weight is 210; thus h_c = 9620 J/g. The atomic percentages of char (CTR minus ash) are given by Baker as:

O = 25.33%	H = 2.18%
C = 69.40%	N = 3.09%

The "model" char is then

$$\text{char} = xC + yC_6H_{10}O_8,$$

where x and y are such that the above ratios are satisfied. From the carbon and hydrogen fractions, x $\approx$ 12 and y $\approx$ 0.5 are obtained; nitrogen is ignored. Upon burning the char,

$$12C + 0.5\ C_6H_{10}O_8 + nO_2 \rightarrow (15 - f)\ CO_2 + f\ CO + 2.5\ H_2O$$

In order to determine f, one more relationship is needed. This is obtained by examining the energy produced. We assume complete combustion of the mucic acid,

$$0.5\ C_6H_{10}O_8 + 4.5\ O_2 \rightarrow 3\ CO_2 + 2.5\ H_2O,$$

and incomplete combustion of the carbon:

$$12C + (n - 4.5)O_2 \rightarrow (12 - f)CO_2 + f\ CO$$

The heat of combustion of C (to CO_2) is 393.5 kJ/g mole (32.77 kJ/g), while the heat of combustion of CO is 283.0 kJ/g mol (23.57 kJ/g), so that the heat of partial combustion (C to CO) is the difference, 110.5 kJ/g mol. With these assumptions, the entire char produces

$$G = 12(393.5) - 283.0\,f + 0.5(2021)\ J$$

The molecular weight of this model char is 249. Thus the heat produced in combustion is

$$h_c = G/249\ J/g$$

The mean heat of combustion of the tobacco, as measured by Sandusky, is

$$\langle h_c \rangle = 17360 \pm 210\ J/g.$$

Therefore, $f = 5.0 \pm 0.18$, and $n = 11.75$.

Thus the CO/CO_2 ratio is $f/(15\text{-}f) = 0.5$. This is typical for smoldering, though very large in comparison with the ratio in flaming combustion.

Note that even though there is only 1 mole of $C_6H_{10}O_8$ for every 24 moles of C, its heat of formation contributes 23% to the overall heat of combustion, a quite significant fraction of the energy balance. The overall model reaction, finally, is

$$12C + 0.5\ C_6H_{10}O_8 + 11.75\ O_2 \rightarrow 10CO_2 + 5CO + 2.5\ H_2O \qquad (83)$$

3. Regression (Burning) Rate

This study only considers the quiescent phase of smoldering, *i.e.*, between puffs, since that is the situation when the cigarette lies on the substrate. The paper in commercial cigarettes is chemically treated so that it decomposes and burns at the same velocity as the tobacco during these quiescent periods; this occurs in a region on the order of 1 mm in width. This location is called the "paper burn line," and will serve as the origin of coordinates ($x = 0$) in our further work. It is assumed here that the reactions in the paper do not influence the tobacco reactions, although we realize that there may well be both thermal and oxidative interaction.

Cigarettes vary within a factor of about two in the speed of propagation of the smolder wave. The average cigarette tobacco column is about 7.3 cm long, and it takes 15 ± 5 minutes to be consumed, without drawing or puffing on it. The burning rates have been measured to lie between 40 and 85 mg/min, consistent with the value given in Section III.B.1. The regression velocity is thus

$$V_r = L/\tau = 5.4 \pm 1.8\ mm/min.$$

The variations depend, at least, on the cigarette radius, the packing density, whether the tobacco leaf has been expanded or not, the moisture content of the tobacco, and the kind of paper, its permeability, and how it has been chemically treated. Note that the moisture content does <u>not</u> affect its peak temperatures (M. Samfield, 1986). Rather, it affects the burning velocity, because it takes time and energy to evaporate the water.

4. Reaction Rates

As will be seen in Section III.D.2, the reaction rates in combustion are well represented by Arrhenius expressions, which can give enormous rates at high temperatures. What limits the reaction rates is primarily the availability of oxygen; that, in turn, depends upon the rate at which the oxygen can be transported into the combustion (Ohlemiller, 1985). Therefore, the rate at which oxygen is allowed to diffuse into the cigarette is the principal determiner of the burning rate, unless the coal is so cooled locally as to cause limitations from the kinetics. The diffusion of oxygen will be discussed further in Section III.B.9.

The mean reaction rate for the cigarette is

$$<RR> \approx 0.85m/V\tau,$$

where 0.85m is the combustible fraction of the tobacco mass, V is the volume of the tobacco column, and τ the total duration of the smolder. We use a nominal mass of m = 1 g. The volume is $V = \pi R^2 L$, where the average L = 7.3 cm and R $\approx$ 0.4 cm; finally, $\tau \approx$ 840 s. Then $<RR> \approx 0.28$ mg/cm^{3}s.

If the reaction rate is described by an Arrhenius expression, then it must be highly peaked in the high-temperature region. Indeed, the simple approximation of an infinitely high reaction rate occurring over a surface which is a paraboloid (or conoid) of revolution might be expected to have some validity. This approach was used by Gugan (1966). Since the actual reaction rate is finite, this "surface" is in fact a thin region. This shell-like region is shown in Figure 17 (taken from Baker (1975)) by the shaded paraboloid. The highest temperatures occur at the centroid of this shell. Thus, suppose an observer were positioned at x = 0, *i.e.*, at the paper burn line. As time progresses and the smolder wave moves to the left, the peak reactions occur in a contracting ring, starting at the periphery and contracting to a point, leaving ash on the outside of the ring.

5. Heat Production Rate

We have seen that the mean mass loss rate is about 60 mg/min for a 870 mg cigarette; hence something like 70 mg/min for a 1 g cigarette. Of this, about 70% is evaporated/pyrolyzed with low energy production or loss, 30% is lost by char oxidation, a highly exothermic reaction. That is, about 20 mg/min are being oxidized this way. With $R_{CO} \approx$ 17 kJ/g, we end up with an energy production rate of about 340 J/min, or about 5.7 W. Note that with the variations among cigarettes described above, this value could easily be 50% greater or smaller:

$$<\dot{Q}> \approx 5.7 \pm 2.8 \text{ W}$$

6. Energy Balance

This heat input is balanced by losses; without going into detail, we can estimate:

a. Enthalpy loss *via* outgassing: $\dot{Q}_e \approx 2.0 \pm 0.4$ W

b. Convective losses from the surface: $\dot{Q}_c \approx 1.7 \pm 0.4$ W

c. Radiative losses from the surface: $\dot{Q}_r \approx 2.1 \pm 0.4$ W

As we see, although the energy losses balance the energy production, the uncertainties in these estimates are very large indeed.

d. Conductive losses: These apply when the cigarette is in contact with a substrate, and are discussed in Section IV. For the "free" cigarette (that is, the cigarette quietly smoldering in wind-free air, distant from any substrate or wall), there are no conductive losses.

7. Distributions Within the Cigarette

Temperature. A representative temperature distribution in a smoldering cigarette is shown by the isotherms in Figure 17. Figure 21, also taken from Baker (1975), shows the measured volume percentage of oxygen. Note that this value is essentially zero in the region of maximum temperature, so that the reaction (oxidation) rate there is low, in spite of the high temperature.

In order to be able to calculate the heat flux delivered to the substrate, the distribution of surface temperature must be known. In particular, most important is the **peak** surface temperature, T_p. Unfortunately, it is not an easy quantity to measure. Indeed, it is not even a well-defined quantity, since (as is seen from Figures 17 and 19) the gas and the solid temperatures are not quite the same.

Moreover, the result depends on the measurement technique. Baker's measurements yielded peak surface temperatures of about 550 °C. Egerton *et al.* (1963) found 616 °C for T_p. Lendvay and Laszlo (1974), using an IR technique, found that $T_p \approx 600$ °C. We will take this to be the mean value. Since peak surface temperatures may well vary by 50 °C among cigarettes, the peak surface temperature is 600 ± 50 °C.

Oxygen. The oxygen concentrations in the freely smoldering (*i.e.*, away from the substrate, in quiescent phase) cigarette are shown in Figure 18. It can be seen that the smoldering is indeed cylindrically symmetric. In fact, in our model it will maintain that symmetry even when interacting with the substrate. Consistent with an oxygen-diffusion-controlled process, the oxygen concentration in the center drops to very low values. The peak reaction rates generally occur in the region where the mole fraction of oxygen, $x(0_2)$, is less than one percent. One can write down some plausible analytic expressions for the radial distribution; but the actual distribution yields some surprises, as can be seen from Figure 18. For example, although one would *a priori* expect the concentration to increase monotonically from the center towards the boundary, examination of the actual dependence along a slice at $z = +6$ mm shows unexpected maxima and minima.

Gas Velocity. Some simple estimates show that the radial outflow velocity of hot gases from the cigarette can be as high as 7 cm/s. Thus inward oxygen diffusion is a counterflow problem. Indeed, this suggests that the principal inflows would be through the ash, away from the paper-burn line, and then axially towards the reaction zone. Note that the buoyancy of the hot gases will in fact affect the gas flow.

Surface Heat Flux. Consider Figure 19, giving the measured temperature of the cigarette surface, parallel to its axis. The net convective flux from this surface to the ambient is

$$\phi_c(x,t) = h[T(x,t) - T_a] \tag{84}$$

Similarly, the net radiative flux is

$$\phi_r(x,t) = \epsilon_C \sigma[T^4(x,t) - T_a^4] \tag{85}$$

where ϵ_c is the emissivity of the cigarette surface, σ is the Stefan-Boltzmann constant, and T_a is the ambient temperature. These fluxes, when integrated over the cigarette surface, must yield the energy loss rates $\dot{Q}_c$ and $\dot{Q}_r$ given in Section III.B.6.

The heat flux from the escaping hot gases, *i.e.*, the enthalpy loss, can be calculated once we have u_r, the radial convective velocity, as a function of x. Upon integration over the surface, it then yields the total enthalpy loss, $\dot{Q}_e$.

8. Pressure

Upon drawing on a cigarette, a person will generate a (negative) pressure corresponding to several hundred Pa (several centimeters of water, where one atmosphere corresponds to 101 kPa and 10.4 meters of water.) In the quiet state, the pressure difference is positive, but a minute fraction of this value. This pressure difference can be estimated:

The flow through a packed bed follows Darcy's law,

$$\dot{m}'' = f\Delta p \tag{86}$$

But

$$\dot{m}'' = \rho_g u_r, \tag{87}$$

where ρ_g is the gas density at the surface and u_r is the radial velocity. ρ_g is given by the ideal gas law,

$$\rho_g = \rho_a T_a / T_g \tag{88}$$

Hence,

$$\Delta p = \frac{u_r}{f}\frac{\rho_a T_a}{T_g} \tag{89}$$

With $u_{max} \approx 0.07$ m/s, $\rho_a = 1177$ kg/m^3, and $T_g \approx 900$ K $\approx 3T_a$, we have:

$$\Delta p \approx \frac{7\times 1.2\times 10^{-2}}{3f} \quad \textit{Pascals}$$

Sandusky (1976) estimates that for peripheral flow, $f \approx 10^{-3}$ s/cm. Hence:

$$\Delta p \approx 30 \text{ Pascals}$$

One atmosphere is 101 kPa, so this corresponds to 3×10^{-4} atm, or about 3 mm of water equivalent.

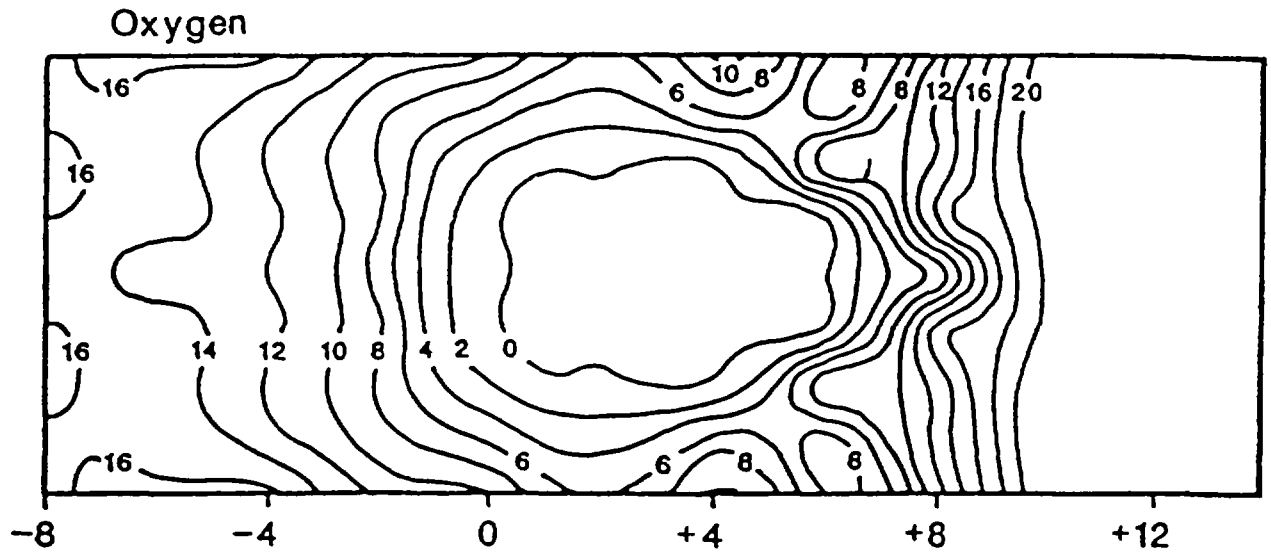

Figure 18. Oxygen concentration in the freely smoldering cigarette during quiet, steady burning.

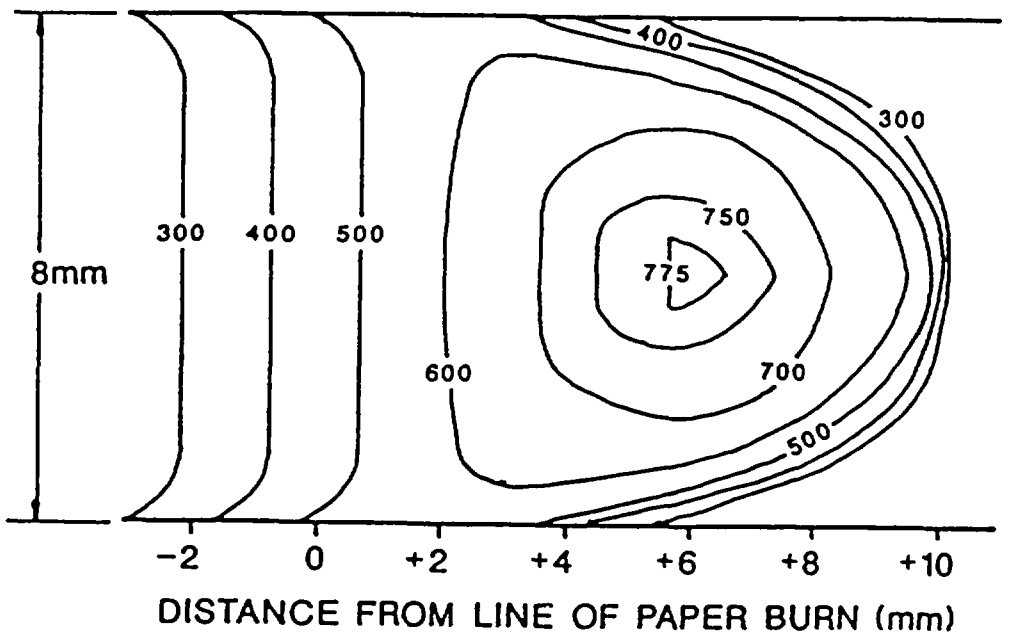

Figure 19. Isotherms in the solid part of the cigarette during quiet, steady burning.

9. Gas Transport

There is a boundary layer surrounding the cigarette, within which the oxygen concentration drops as the surface is approached. Fresh air is supplied by the ambient *via* convection and diffusion, as indicated by the arrows in Figure 20. That the oxygen must transport inward is clear, since the volume of air needed to consume the cigarette is about 1000 times the volume of the solid. Thus, 99.9% of the oxygen needed for combustion of the cigarette must come from the ambient. Some part may be drawn in from (through) the substrate, when the cigarette is in contact with it, but that is estimated to be a small fraction of what is drawn in from the atmosphere Ohlemiller *et al.* (1993, Appendix C), and it has not been modeled here. If there were no substrate, the inward diffusion would be approximately symmetric, the only deviation from symmetry being caused by the upward gas flow due to buoyancy.

Although the cigarette paper is permeable, it largely inhibits the diffusion of oxygen from the air into the tobacco, so long as it is intact. Once it has burned, its resistance to oxygen diffusion is much diminished. Since no measurements of this residual resistance have been published, we assume that it is zero. Therefore, most of the oxygen which is needed to sustain combustion diffuses into the cigarette in front of the paper burn line. [Not all of the needed oxygen is drawn in that way, however. If the paper is made non-porous, the cigarette will self-extinguish.]

Similarly, the considerable gradient in CO_2 which is established by combustion means that there is simultaneous outward diffusion of CO_2. Stoichiometrically, each molecule of O_2 reacts with a single carbon atom. This is how the cigarette loses most of its remaining mass upon combustion (recall that 60% of its mass, at a given point, already disappeared during dehydration and pyrolysis). Some of this mass is convected out, and some of it diffuses out, as just described. It is not difficult to show that the convection rate is one to two orders of magnitude greater than the diffusion rate. Note, to begin with, that before there is any counterflow diffusion of oxygen, about 60% of the tobacco column mass evaporates/pyrolyses away. This process occurs just adjacent to the combustion region. Thus at least 2/3 of the total outflow is due to convection.

10. Diffusion Coefficients

The diffusion that we are concerned with is that of O_2 in N_2. We will call the diffusivity of O_2 in N_2, D_o. For porous media, the effective diffusivity depends on the porosity, or the void space. It is shown in Szekely *et al.* (1976) that

$$D_{eff} / D_o = 0.677\, \Phi^{1.18} \tag{90}$$

for $\Phi < 0.7$. Although the total void fraction is $\Phi = 0.85$ (Muramatsu, 1981), we use this relationship nevertheless. We thus obtain the effective diffusion coefficient

$$D_{eff} \approx 0.56\, D_o = 0.112 \text{ cm}^2/\text{s}$$

at ambient temperature. This is precisely the value used by Muramatsu (1981). The diffusion coefficient is assumed to be the same for all the gases.

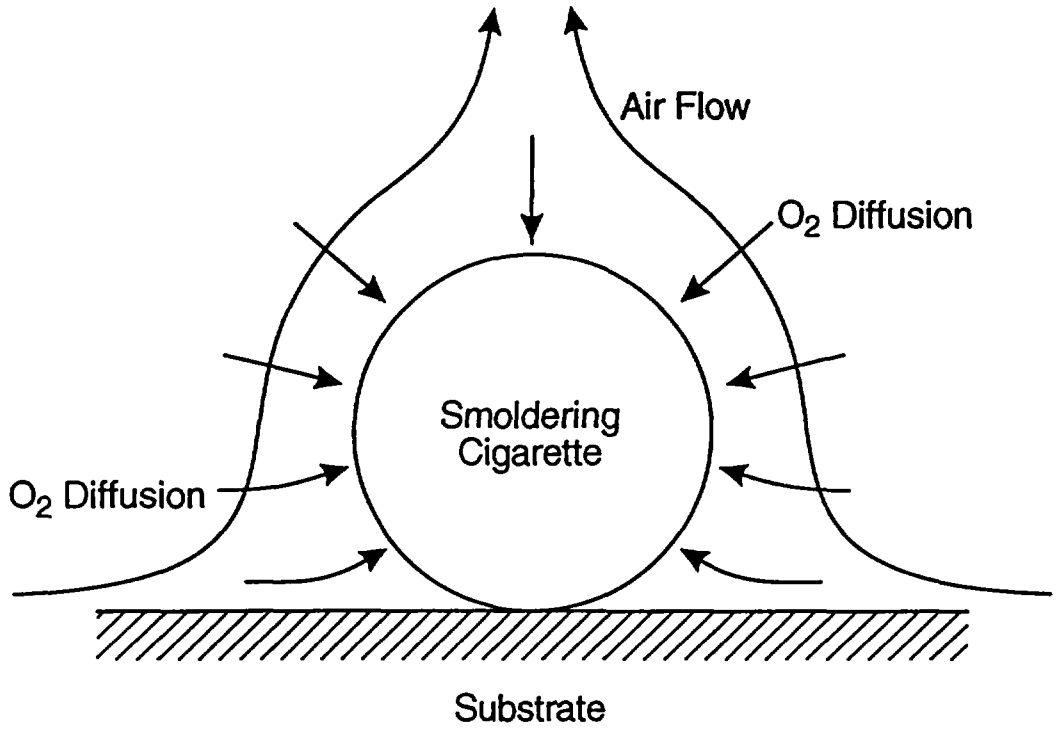

Figure 20. Schematic of how air enters the smoldering cigarette when it is resting on a surface.

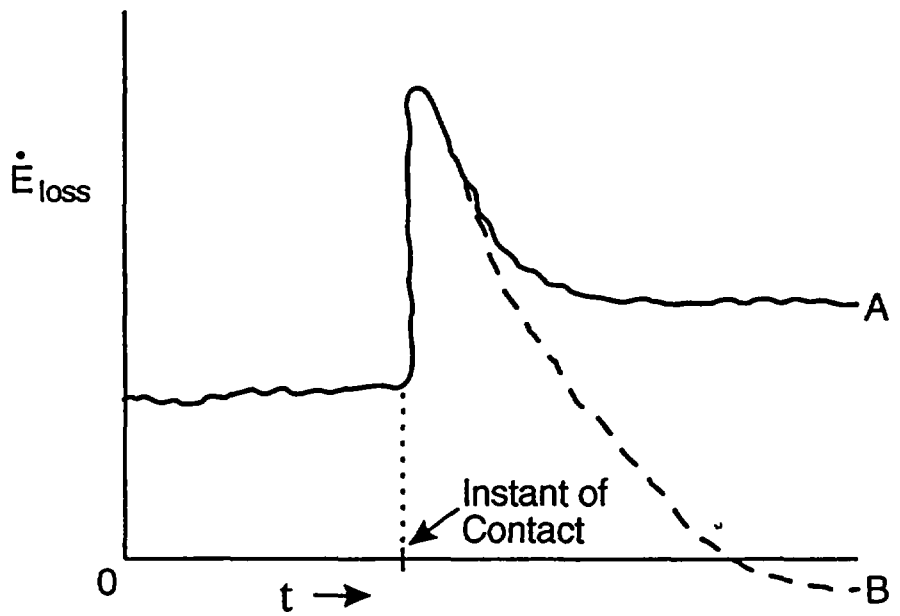

Figure 21. Schematic of the energy losses of a smoldering cigarette as a function of time, when it is dropped onto a surface. Curve A corresponds to a dense, inert substrate. Cuve B corresponds to a substrate which undergoes exothermic reactions.

From equation (16.3-1) of Bird *et al.* (1960), we find that for O_2 in N_2, the temperature dependence is

$$D_o(T) = 0.199\left(\frac{T}{293.16}\right)^{1.823} \quad \text{cm}^2/\text{s} \tag{91}$$

We shall use the same coefficient, but the theoretical temperature dependence

$$D_e = D_o(T/273)^{7/4} \tag{92}$$

rather than the empirical relation above.

11. Conduction Losses

These apply when the cigarette is in contact with a substrate, the situation of concern in actual fire initiation. According to the estimates made in Gann *et al.* (1988), the initial power loss to the substrate is about 2.1 ± 0.35 W, going down to about one-third of this in the steady state.

C. PREVIOUS MODELING EFFORTS

A number of attempts have been made to model the isolated smoldering cigarette or similar object. All of these attempts make some simplifying assumptions in order to make the problem tractable.

An early, related model is due to Moussa *et al.* (1977). They experimented with, and then modelled, the smoldering and extinction of a cellulose cylinder without any paper wrapping. They assumed the smoldering to be steady-state, and they treated the problem as one-dimensional (*i.e.*, no radial gradients). They found, experimentally,

- the smoldering velocity to be closely related to the maximum temperature in the cylinder;
- reasonable agreement between theory and experiment for the extinguishment limit;
- the rate-limiting step in the combustion to be diffusion of oxygen to the char, which is in good accord with experiment.

They also calculated values for v, the propagation velocity of the smolder wave. However, that calculation depends on an uncertain parameter, and the overall accuracy of the model is questionable.

A much more realistic and detailed model of a cigarette was produced by Sandusky (1976) and by Summerfield *et al.* (1978). It is also a one-dimensional model, but it considers the steady-draw case, rather than the free-burn condition. The model is heterogeneous; that is, it explicitly takes into account the fact that the tobacco comes in shreds. It considers a two-step process: pyrolysis to a char, followed by the oxidation of the char. It ignores water evaporation. The char-oxidation reaction is assumed to be a linear function of the oxygen concentration. The combustion model is time-dependent rather than steady-state, and considers the cover paper indirectly, via a varying surface permeability to oxygen. It uses a sophisticated treatment of heat transfer inside the cigarette, including heat transfer by radiation as well as by solid phase conduction.

The model consists of ten simultaneous, coupled partial differential equations (PDEs), and the starting condition assumes the presence of fixed amounts of ash, char, and tobacco. The calculation predicts the burning velocity fairly well, as a function of draw rate. The dependence on oxygen mole fraction in the atmosphere is less well predicted, although this is not important for the current purpose. The calculated gas temperature profile is fairly good: the peak is about right, but the width of the distribution is too narrow. Since it is a steady-draw model, diffusion and natural convection within the cigarette are considered as being of relatively minor importance.

The most elaborate model is that due to Muramatsu *et al.* (1979, 1981); it was developed in two stages. In the 1979 reference, they developed a one-dimensional, steady-state model for the pyrolysis of the cigarette. They focused on the evaporation-pyrolysis zone in a naturally smoldering cigarette. The model considers:

- pyrolysis of tobacco obeying Arrhenius kinetics,
- evaporation of water from tobacco following a mass-transfer and rate-determined process,
- weight loss of tobacco due to pyrolysis and evaporation,
- internal heat transfer characterized by an effective thermal conductivity which includes approximate radiation heat transfer,
- heat loss attributable to free convection and radiation from the outer surface of the cigarette and to endothermicity of the evaporation process, and
- smoldering speed.

These processes are expressed by a set of simultaneous ordinary differential equations that are solved numerically by the Runge-Kutta-Gill method. The equations are ODE's rather than PDE's, since they are independent of t and depend only on x, the position along the axis. The propagation velocity, v, is imposed. They do not include the convection or diffusion of gases other than water vapor. They take the existence of the paper wrapping into account only through its effect on the loss of water vapor.

These approximations work well. The model yields good agreement between theory and experiment for the temperature and density along the axis in the pyrolysis-evaporation region. Thus, the agreement for $T(x)$ and $\rho(x)$ is good for $x < 0$, *i.e.*, before the char-oxidation region, which is not considered in this part of their model. [As in Section III.B, we use $x = 0$ as the boundary between the pyrolysis region and the char-oxidation region, at the surface.] For $x > 0$, the calculated temperature profiles deviate substantially from measured ones, as might be expected. The dependence of the profiles on the imposed velocity shows only semi-quantitative agreement.

In the 1981 Muramatsu work, a char-oxidation model was added to describe the processes occurring in the region $x > 0$. The model is quite detailed; it takes two char oxidation reactions into account and is two-dimensional (cylindrically symmetric). Unlike the Sandusky model, it is a homogeneous model, *i.e.*, it does not take directly into account the fact that there are solid particles and a gaseous medium. Energy loss is through radiation and convection at the outside surface of the cigarette. Again unlike the Sandusky model, it assumes that there is no temperature difference between the solid and gaseous phases. This is not a bad approximation for natural smolder, and simplifies the problem considerably. Heat transport by thermal radiation inside the cigarette is taken into account in a somewhat different way than is done

in Summerfield *et al.* The thermal conductivity at any point is assumed to be isotropic. Similarly, the temperature-dependence of the gaseous diffusivity is taken into account explicitly. Finally, the pyrolysis/evaporation model and the char oxidation model are tied together through an energy-flow matching condition at the pyrolysis/char-oxidation boundary to obtain the appropriate smolder velocity.

The results of calculations made by Muramatsu for six representative cigarettes agree well with experimental data:

- The peak temperatures, when expressed in °C, are only 2.7% to 5.7% higher than the experimental data. [Since the temperature calculations are made with $T_a \approx 20$ °C as the datum, it is appropriate to use degrees Celsius for comparisons.]

- The smolder velocities are 14% high, on the average, varying between 4% low and 26% high.

- The calculated variations of smolder rate (V) and peak temperature (T_m) with R (the cigarette radius), the packing density, ρ_p, and the moisture content in the tobacco shreds are indistinguishable from the experimentally observed variations. The dependence of V and T_m on ambient oxygen partial pressure is not well-predicted; this is not an important consideration in our study.

- The calculated distributions of temperature and oxygen concentration in the char oxidation region are in agreement with measurement, except for a scale factor: the predicted distribution is narrower than observed. Because of this last point, Muramatsu *et al.*'s model cannot be used directly to obtain the flux emitted to the substrate: the too-narrow temperature distribution would substantially underpredict the energy output of the cigarette to the substrate. However, the model is excellent for some purposes; in particular, to estimate cigarette smolder velocities.

Although the model is very good, it may be appropriate to list some of its limitations:

- Prior to decomposition, the paper wrapping is assumed to be impervious to oxygen. According to experiment, this should result in the cigarette going out.

- Perhaps in order to be consistent with the above assumption, radial convection of gases is not included.

- Their calculation uses an iterative procedure to converge to a solution. If the calculation has not converged after 1000 iterations, the unconverged result is nevertheless accepted as correct.

Mitler (in Gann *et al.*, 1988) and Mitler and Davis (1987) developed a detailed, homogeneous model of a freely smoldering cigarette, called CIG25. Unlike Muramatsu's models, it is time-dependent rather than steady-state and two- rather than one-dimensional. Unlike Sandusky's model, diffusion and natural convection within the cigarette are included, since there is no steady-draw convection to overwhelm these effects. We may make some further comparisons; CIG25 differs from the model introduced by Sandusky *et al.* in a number of ways:

- Sandusky's model is heterogeneous, with tobacco shreds embedded in a gas. Therefore the local "ambient" for oxygen varies, and the rate at which oxygen reaches the shred surface is given by

$$k_m(y_o - y_s) \tag{93}$$

where y_o is the local ambient mass fraction of oxygen and y_s is the value at the shred surface.

CIG25 is homogeneous, with the cigarette core being a mixture of "solid" and "gas." The oxygen available to react with the solid is the local value, obtained by solving the diffusion equation for y, the oxygen mass fraction.

- The Sandusky *et al.* model is a steady-draw model with substantial axial convection and no natural smolder; CIG25 considers natural smolder only, and neglects axial convection in comparison to radial convection.

- The Sandusky model is a one-dimensional model which averages over the cross-section. CIG25 is two-dimensional, having radial gradients.

- CIG25 takes only one reaction into account, effectively considering a char cigarette, rather than a real tobacco cigarette.

Of course the models have a number of similarities; for example, they both neglect the production, transport, and effect(s) of water.

Mitler (1988) also described a "semi-empirical" model. This simple version consists of a number of correlations, partly based on results of making parametric runs with Muramatsu's model and corrected by experimental data where possible.

D. MODELING THE CIGARETTE

1. Assumptions

Based on the successes of the prior models, this Section lists the assumptions and equations valuable to a good, yet tractable model of a cigarette on a substrate. CIGARET uses a subset of them and is described in Section III.D.3. The following are facets to be included and their physical forms:

1. The cigarette model is two-dimensional, with axial and radial coordinates. It is also time-dependent, yielding V directly, whether or not it is constant. If a steady state were assumed, then the equations would simplify; however, it would then be necessary to choose the smolder velocity correctly (*i.e.*, as an eigenvalue), as Muramatsu did. Moreover, if the equations are taken to be time-dependent, the heat and mass transfer equations are parabolic partial differential equations (PDE's) which are easier to solve, in some ways. Finally, the convergence for the steady state equations is very slow. Indeed, Muramatsu found that one thousand iterations would not suffice, at times.

2. The cigarette is modeled with one pyrolysis reaction and one char-oxidation reaction.

3. The (internal) gas flow velocities depend on the pressure gradients; since the axial gradients, of order $\Delta p/L$, are generally much smaller than the radial gradients, of order $\Delta p/R$, axial convection is neglected, as being much smaller than radial convection.

4. The water (pre-existing or produced during combustion) in the tobacco column is also ignored.

5. The tobacco column is treated as a homogeneous, uniform mixture of gas and solid; there are no tobacco shreds.

6. The gas and solid phases are at the same temperature, locally.

7. Species or temperature gradients within the tobacco shreds will be neglected, consistent with assumption #5.

8. Radiation transfer within the cigarette is treated as an effective thermal conductivity.

9. The thermal conductivity is the same function of temperature throughout the cigarette, *i.e.*, whether in ash, char or tobacco.

10. The paper behavior appears only in the boundary conditions.

11. Consistent with assumption #10, any (axial or radial) gradients in the paper are ignored; an effective mass transfer coefficient is used to model diffusion through the paper.

12. The gases generated or heated by combustion move radially outward to the side boundary (aside from diffusion). Thus there is a radial flow calculated strictly by mass conservation. The gas pressure within the cigarette is assumed to be only negligibly different from atmospheric, and therefore no momentum equations are written.

13. The gas phase is quasi-steady; that is, $\partial \rho_g / \partial t \approx 0$.

14. No particulate aerosols are produced.

15. The cigarette combustion zone retains its cylindrical symmetry when lying on a substrate. This is observed to be approximately correct for some cigarettes on some fabric/foam substrates, especially after the cigarette "recovers" from the transient cooling effects of the substrate.

16. Prior to its ignition, the substrate's presence has two effects on the cigarette, both of which can be assumed to apply symmetrically (on the average) to the entire cigarette periphery:

    (a) The oxygen supply to the cigarette is reduced by some factor. The degree of reduction will depend on the permeability of the substrate.

    (b) The thermal effects (*e.g.*, as a heat sink) can be calculated in a decoupled manner (this assumption is weak, and may eventually have to be dropped).

It should here be made explicit that this model is for an isolated (that is, not in contact with any surface), quietly smoldering cigarette. Such a model will predict, among other things,

- the external heat flux from it, and the extent of the heating zone,
- the velocity of smolder propagation, and
- how these depend on: the radius of the cigarette (R), the tightness of packing (via the void fraction ϕ), the type of tobacco (*via* its thermophysical and kinetic parameters: heat of gasification H_v, heat of combustion H_c, activation energies and pre-exponential factors, density ρ, thermal conductivity k, specific heat C_p, etc), and the wrapping paper, *via* its permeability and its ignition, or decomposition, temperature. A better model would explicitly include paper thickness, chemical composition, porosity, and kinetic parameters, as well.

2. Governing Equations

The equations which describe the mass and energy transport in a smoldering cigarette will now be presented. Any simplifying assumptions beyond the 16 above will be indicated as each equation is discussed.

It is necessary to clarify some of the terms appearing in the equations. In the decomposition of the tobacco, one gram of tobacco, upon pyrolysis, produces n_c grams of char. The other $1-n_c$ grams are gaseous products. Each gram of char reacts with n_{O2} grams of oxygen to produce some heat, n_A grams of ash, and $1 - n_A + n_{O2}$ grams of gaseous products of combustion. Since the combustion process mostly proceeds at very low oxygen concentrations, it can be expected to be incomplete, and n_{O2} is smaller than the stoichiometric value. In the following equations, x is the axial coordinate.

Mass Conservation.

$$\frac{\partial \rho_s}{\partial t} = -[(1-n_C)R_p + (1-n_A)R_{CO}] \,. \tag{94}$$

where ρ_s is the mass density of the solid, R_p is the pyrolysis rate (in gm/cm^{3}s) and R_{co} the char oxidation rate. Axial convection is dropped, according to assumption #2, and the equation of continuity in cylindrical coordinates becomes

$$\frac{\partial}{\partial t}[\rho_s(1-\phi) + \rho_g\phi] + \frac{1}{r}\frac{\partial}{\partial r}(\phi r \rho_g u_r) = 0 \tag{95}$$

where r is the radial coordinate, ρ_g is the mass density of gases, ϕ is the void fraction in the cigarette (*i.e.*, the volume fraction of gas, rather than of tobacco shreds), and u_r is the radial velocity of the gas. Since the shreds are assumed not to shrink, ϕ remains constant. Assumption #11 implies

$$\frac{\partial}{\partial t}(\phi\rho_g) = \phi\frac{\partial \rho_g}{\partial t} \approx 0 \tag{96}$$

and using equation (95), the gas equation results:

$$\frac{\phi}{r}\frac{\partial}{\partial r}(r\rho_g u_r) = (1-\phi)[(1-n_C)R_p + (1-n_A)R_{CO}] \tag{97}$$

Momentum. The procedure used in CIGARET is to assume no pressure difference so that the ideal gas law is satisfied. Mass conservation then gives the velocities directly, *via* the gas equation, Equation (97). The reason is that any attempt to calculate the convective outflows and velocities from a calculated pressure difference would require that we know the coefficient in Darcy's law (Section III.B.9) very well, *and* that we accurately calculate very small differences of large numbers. That would be extremely demanding of the computation and possibly prohibitive.

Species. V is the total volume of the cigarette; the total volume occupied by the solids in the cigarette is

$$V_s = (1-\phi)V$$

We define the mean densities

$$\rho_i \equiv m_i/V_s \qquad i = A, C, T \tag{98}$$

where A, C, and T stand for ash, char, and tobacco, respectively. In this equation, m_A = total mass of ash, etc. Then the cumulative density of the solid parts of the cigarette is

$$\rho_S = \rho_A + \rho_C + \rho_T \tag{99}$$

Each of these densities varies with time.

The equations for the changes in tobacco and char densities are

$$\frac{\partial \rho_T}{\partial t} = -R_p \tag{100}$$

and

$$\frac{\partial \rho_C}{\partial t} = n_C R_p - R_{co} \tag{101}$$

The ash is inert and simply accumulates, so that an equation for ρ_A is not required.

Oxygen. We must know the oxygen concerntration everywhere in order to calculate the char-oxidation rate. The other gases are inert or nearly so. Moreover, the gases and solids are assumed to have the same temperature, so there is no energy exchange, and we do not need to consider the CO_2 diffusing out. Therefore, of the gaseous species equations, it is only necessary to include that for oxygen. Rather than dealing with the oxygen density ρ_{O2}, the equations are best written in terms of y, the oxygen mass fraction:

$$y \equiv \rho_{O_2}/\rho_g \tag{102}$$

The equation is

$$\rho_g \frac{\partial y}{\partial t} + \rho_g u_r \frac{\partial y}{\partial r} = \frac{\partial}{\partial x}\left(\rho_g D_e \frac{\partial y}{\partial x}\right) + \frac{1}{r}\frac{\partial}{\partial r}\left(r \rho_g D_e \frac{\partial y}{\partial r}\right) - \left(\frac{1-\phi}{\phi}\right)\{y(1-n_C)R_p + [y(1-n_A) + n_{O_2}]R_{CO}\} \tag{103}$$

where D_e is the oxygen diffusion coefficient, and the axial convection term has been dropped.

Energy. Assuming that the gas is quasi-stationary, as in assumption #12 above, and that the specific heats of all gases are the same and independent of temperature, then the energy conservation equation can be written in terms of the temperature. It is:

$$(1-\phi)\rho_s C_s \frac{\partial T}{\partial t} + \phi \rho_g u_r C_g \frac{\partial T}{\partial r} = \frac{\partial}{\partial x}\left(k\frac{\partial T}{\partial x}\right) + \frac{1}{r}\frac{\partial}{\partial r}\left(rk\frac{\partial T}{\partial r}\right) + (1-\phi)(Q_{CO}R_{CO} - Q_p R_p) \tag{104}$$

where
C_s = specific heat of the solid
C_g = specific heat of the gases
k = thermal conductivity of the cigarette (see assumption #8)
Q_{co} = energy released from char oxidation (lower heat of combustion)
Q_p = energy absorbed in (endothermic) pyrolysis

The internal heat transfer has a radiative and a conductive component, as described earlier. The expression used here is the same as that used in Muramatsu (1981) and is due to Kunii (1961); for porous materials,

$$k(T) = (1 - \Phi^{2/3})k_s + \Phi^{1/3}\left(k_g + \frac{2}{3}h_r D_p\right) \tag{105}$$

where h_r is a heat transfer coefficient for radiation:

$$h_r = \epsilon_T 4\sigma T^3 \tag{106}$$

D_p is the mean pore diameter, Φ is the total void fraction (including the void space in the shreds, and is therefore larger than ϕ), ε_T is the emissivity of the shreds, k_g is the thermal conductivity of the gas, and k_s that of the solid shred (and depends on the shred's mass density).

Since the gas pressure in the quiescent cigarette is very nearly the ambient air pressure, and since there is not a great difference between the molecular weight of the product gases and air, the ideal gas law permits one to write the gas density in the form

$$\rho_g = \rho_{go} T_o / T \tag{107}$$

where T is the absolute temperature.

Reactions. Finally, expressions for the tobacco and char reaction rates are needed. It is assumed that each is given by an Arrhenius relation:

$$R_p = \rho_T^m Z_p \exp(-E_p/RT) \tag{108}$$

where the exponent m is to be determined experimentally, as is the "frequency factor" (or "pre-exponential factor") Z_p. E_p is the activation energy for the pyrolytic reaction and R is the universal gas constant. The tobacco density ρ_T may be expressed as

$$\rho_T = \rho_S y_T \tag{109}$$

where y_T is the tobacco mass fraction.

Similarly, the char-oxidation reaction rate is taken to be

$$R_{CO} = \rho_C^n \rho_{O_2}^p Z_{CO} \exp(-E_{CO}/RT) \tag{110}$$

where (again) the exponents n and p are to be determined experimentally, and the densities are written in terms of the respective mass fractions:

$$\rho_c = \rho_s y_c \qquad \text{and} \qquad \rho_{O2} = \rho_g y \tag{111}$$

Initial Conditions. Before ignition of the cigarette, the initial conditions are

$$\rho_S(x,r,0) = \rho_{so} = \rho_{To} \tag{112a}$$
$$\rho_C(x,r,0) = \rho_A(x,r,0) = 0 \tag{112b}$$
$$T(x,r,0) = T_o \tag{112c}$$
$$y(x,r,0) = y_a \ (= y_{ambient} = 0.232) \tag{112d}$$

For the calculations, however, it was assumed that a match had been applied to the x = 0 end of the cigarette, producing some reactions. These used up only a small fraction of the tobacco, but most of the oxygen that had been *in situ*. The initial temperature distribution was assumed to be very high (1000 K) in the first millimeter of the tip, then to decrease linearly to ambient temperature in the next millimeter.

The oxygen mass fraction behaves in complementary fashion, as follows. For the following calculation, we may ignore the stoichiometry developed earlier and simply assume that the combustion of char proceeds according to

$$C + [(1+a)/2]\,O_2 \rightarrow a CO_2 + (1-a)CO$$

Then 16(1+a)/12 grams of oxygen are needed to burn one gram of carbon (char). As combustion lowers the local mass fraction of oxygen from y_a to y, it will lower the relative density of char (and hence tobacco) from 1 to x, where

$$x = 1 - [0.75/(1+a)n_c](\rho_g/\rho_T)(y_a - y)$$

This permits us to enter the initial density of tobacco so that it is consistent with the assumed distribution of $y(O_2) = y$. ρ_o is the actual mean tobacco density in the virgin cigarette.

Boundary Conditions. On the axis,

$$\left(\frac{\partial y}{\partial r}\right)_{r=0} = \left(\frac{\partial T}{\partial r}\right)_{r=0} = 0 \qquad \textit{for all } x, t \tag{113}$$

At the lit end of the cigarette, the temperature boundary condition is:

$$k\left(\frac{\partial T}{\partial x}\right)_{x=0} = \epsilon_A \sigma (T^4 - T_a^4) + h_e (T - T_a) \tag{114}$$

for all r and t. $T = T(0,r,t)$ and $T_a = T_{ambient}$.

Here, too, h_e = convective heat transfer coefficient (at the end), σ is the Stefan-Boltzmann constant, and ϵ_A = emissivity of the cigarette at the $x = 0$ end. We are assuming a grey body. The value to be used here should be that of the tobacco ash. It is assumed that the ash never falls off the cigarette, not realistic for active smoking, but appropriate for the case when the cigarette rests on a substrate. Moreover, if it were not made, the geometry would be continually changing, and the boundary conditions would become exceedingly complicated.

There is usually a filter at the other ($x = L$) end. It has been observed that the presence of a filter increases ignition propensity (Gann *et al.* 1988). This is probably due its limiting axial flow of air through the tobacco column. This model presumes no such flow. Thus, for the temperature boundary condition at the other end,

$$-k\left(\frac{\partial T}{\partial x}\right)_{x=L} = \epsilon_T \sigma (T^4 - T_a^4) + h_e (T - T_a) \tag{115}$$

for all r and t (where now $T = T(L,r,t)$).

Next, the cigarette's side surface must be considered. It is covered by paper. This paper wrapper in principle should also be included with its own set of equations, which include its reaction kinetics. However, the amount of heat released when it burns is negligible in comparison to that released by the tobacco. If a unique paper decomposition or ignition temperature can also be specified, then the paper's kinetic equations can be replaced by two appropriate boundary conditions, which simplifies the problem considerably.

If there were no paper, then the temperature boundary condition at the sides would be

$$-k(x,R)\left(\frac{\partial T}{\partial r}\right)_{r=R} = \epsilon_c(x) \sigma (T^4 - T_a^4) + h(T - T_a) \tag{116}$$

The emissivity of the cylinder surface is different for ash, char, or virgin material (except at the tip, the relevant material is paper, rather than tobacco, as is pointed out below); thus the emissivity is a function of x. Also, the thermal conductivity at the surface will in general depend on whether it is ash, char, or virgin material. The assumption which is made here is that k is the same for all three (assumption #9).

Similarly, although the heat transfer coefficient at the sides, h, will be different from what is at the ends, we simplify by assuming that

$$h_e = h$$

Moreover, since the ends generally emit much less heat than do the sides, it is not so important that we use the exactly correct values there. The emissivity ε_c has one value for the virgin region, another for the char region, and a third for the ash region. Note that these refer to *paper* char and ash, and may occur at different temperatures, and therefore different locations, than for the just-underlying *tobacco* char and ash. Because of these differing emissivities, ε_c will vary along the surface. Although $\varepsilon_c(x)$ may be a continuous function, the simplest approximation that can be made is that the paper pyrolyses, ignites, and disappears at some paper ignition temperature T_{ip}, so that there are just two values for ε_c - that for the virgin paper and that of ash. These meet at the paper burn "line." Experiments (Sandusky, 1976) have shown that $T_{ip} \approx 450 \pm 100$ °C.

The peak surface temperature occurs towards the "tip" end of the cigarette (*i.e.*, at $x < 0$), and therefore it is most important that ε_A be accurately chosen.

Finally, the oxygen boundary conditions must be considered. It is assumed, for the sake of simplicity, that the filter prevents any oxygen diffusion at the cold end ($x = L$):

$$D\left(\frac{\partial y}{\partial x}\right)_{x=L} = 0 \tag{117}$$

where D is the diffusion coefficient for oxygen within the cigarette. At the other end, the conditions must be

$$D\left(\frac{\partial y}{\partial x}\right)_{x=0} = \gamma_b (y_a - y_e) \tag{118}$$

where $y_e = y(0,r,t)$ is the oxygen mass fraction at the "hot" end of the cigarette and y_a is the ambient fraction, defined in equation (112d). D is a function of temperature; for the sake of simplicity, it is assumed that it is the same function for ash as it is for virgin tobacco and for char. γ is the mass transfer coefficient, sometimes referred to as k_g or k_m; see, for example, equation (93). Muramatsu (1981) gives it as

$$\gamma_b = 6.38 \times 10^{-3} \left[\frac{T^{2.75}(T - T_a)(T + 123.6)}{R T_a}\right]^{1/4} \quad \text{cm/s} \tag{119}$$

for the effect of the boundary layer, where T is the mean value between T_c (the local cigarette surface temperature) and T_a (the ambient temperature), and all temperatures are in Kelvins. This holds for the free cigarette, where there is no blockage by a substrate

For the side surface, the counterflow convection must be taken into account:

$$D\left(\frac{\partial y}{\partial r}\right)_{r=R} - u_r y_s = \begin{cases} \gamma (y_a - y_s) & x \geq x_p \\ \gamma_b (y_a - y_s) & x < x_p \end{cases} \tag{120}$$

where $x_p = x_p(t)$ is the position of the paper burn line at time t, u_r is the (outward) radial velocity at the surface, and y_s is the oxygen mass fraction at the surface.

The paper resistance to oxygen diffusion can be expressed as

$$\gamma_p = D_p/\delta \tag{121}$$

where D_p is the diffusion coefficient in the paper and δ is the mean paper thickness. The total resistance of both paper and boundary layer is then

$$\gamma = (\gamma_b^{-1} + \gamma_p^{-1})^{-1} \tag{122}$$

According to equation (120), the remains of the paper wrapper, where the paper has burned, present no barrier at all, and the radial oxygen diffusion at the boundary depends only on the properties of the boundary layer.

It is instructive to make estimates for the magnitudes of these terms. From equation (106), we see that at the peak surface temperature, 600 °C, $D_e \approx 0.856$ cm^2/s. For the gradient, we see that $x(O_2) \approx 0$ to about halfway out along the radius, so that we can take

$$\frac{\partial y}{\partial r} \sim \frac{y_s - 0}{R/2} \tag{123}$$

For γ, we use $\gamma \approx 0.8$ cm/s (from Table 5-B-1, Gann *et al.*, (1988)). Then equation (120) relates u_r and y_s. From Figure 18 (Figure 5-3b in the same reference), $[O_2]_s = 8 \pm 2\%$ in the most active region. Therefore, $y_s \approx 0.09 \pm 0.02$. Hence,

$$u_r \approx \frac{2D}{R} - \gamma\left(\frac{y_a}{y_s} - 1\right) \approx \frac{0.856}{0.2} - 0.8\left(\frac{0.232}{.09 \pm .02} - 1\right) = 2.9 \pm 0.5 \quad \text{cm/s}$$

If the gradient is indeed given by equation (123), then in order to be able to satisfy equation (120), we must have

$$u_r < 2D/R. \tag{124}$$

That is, too large a radial convective flow will prevent any oxygen from being able to enter the cigarette through the sides. This quantitatively confirms our physical intuition.

3. Choices for CIG25

The model CIG25 used a subset of the above equations which was believed to capture the most important processes. The key simplifications were:

- Since the pyrolysis is only weakly endothermic, it was dropped -- that is, it was assumed that $R_p = 0$ in equations (97), (101), (103), and (104).
- Probably more limiting, it was assumed for simplicity in some parts of the program that ρ_c and ρ_g are constant and uniform. In other parts of the program, the ideal gas law was properly used; hence, the relationships were inconsistent.
- There was no boundary condition for convective flow. This was not a serious issue, although the intact paper forms a barrier against convection. However, since there is no pyrolysis in this model, the only place where gas flow can originate is where high

reaction rates occur, producing high temperatures and expanding gases. All this takes place largely in front of the paper burn line, and therefore one would not expect significant flow behind that line. Therefore there was no need for such a boundary condition.

- The radiative losses from the surface were linearized (see equation (131)).

Because this was only a "partial" model, we would expect the results obtained with the correct values of input parameters to be somewhat unrealistic. The input parameters therefore have to be modified, in order to compensate for this.

E. NUMERICS

1. Discretization of the Equations

For the numerical calculations, the cigarette is divided into 10 or 20 cylindrical shells, *i.e.*, $\Delta r = 0.4$ or 0.2 mm, and into slices of the same thickness, $\Delta x = \Delta r$. This last equality makes the expressions a little simpler and more compact.

Originally, the equations were discretized using central differences for the spatial derivatives. This gives simple expressions which are accurate to second order in Δx. However, it is easy to show (*e.g.*, Peyret and Taylor (1983), Chapter 2) that this approximation introduces an artificial (*i.e.*, numerical) diffusion term with a negative sign. Hence, if the actual diffusion term is not large enough, numerical oscillations will begin, and instability ensue.

The stability criteria for the homogeneous convection-diffusion equation

$$\frac{\partial f}{\partial t} + A\frac{\partial f}{\partial x} + B\frac{\partial f}{\partial y} - D\nabla^2 f = 0 \tag{125}$$

are

$$\Delta t \leq \frac{4D}{|A|^2 + |B|^2} \tag{126}$$

and

$$\Delta t \leq \frac{\Delta x^2}{4D}, \tag{127}$$

assuming that $\Delta y = \Delta x$. Equation (126) is the Courant criterion.

Care was taken to satisfy the constraints on Δt and on the magnitude of the mass diffusion coefficient. Nevertheless, severe oscillations arose within a few hundred time steps. This was traced to the inhomogeneous source terms. Thus, when the convective-diffusive equation we are solving has a source term, that invalidates the criteria for Δt found above. The source terms are of Arrhenius type, and produce considerable stiffness in the equations. It would have been necessary to constrain Δt to a microsecond or so in order to avoid these oscillations. These problems could have been overcome by using implicit solution schemes and/or operator-splitting methods (Wichman, 1991). Another approach which is often used is to quasi-linearize the equations. This, however, would have reduced the accuracy

of the solutions. Thus, it was decided to use the same numerical technique as is used in CIG25. It is described in Section III.E.2.

If one takes $\Delta x = 0.2$ mm, then with the present DIMENSION statements, that only allows for cigarettes of 30 mm length (ordinary cigarettes average about 73 mm). However, it is likely that a quasi-steady state or ignition would develop long before 30 mm of cigarette was consumed.

2. Method of Solution

Ames (1969) shows that an equation of the form

$$\frac{\partial^2 u}{\partial x^2} + f(x,t,u)\frac{\partial u}{\partial x} + g(x,t,u) = p(x,t,u)\frac{\partial u}{\partial t} \tag{128}$$

can be put into the Crank-Nicolson form as follows:

$$\frac{1}{2h^2}\delta_x^2[u_i^{j+1} + u_i^j] + \frac{1}{4h}f[ih,(j+1/2)k,(u_i^{j+1} + u_i^j)/2]\delta_x(u_i^{j+1} + u_i^j) +$$

$$g[ih,(j+1/2)k,(u_i^{j+1} + u_i^j)/2] = p[ih,(j+1/2)k,(u_i^{j+1} + u_i^j)/2]\frac{(u_i^{j+1} - u_i^j)}{k} \tag{129}$$

where δ_x is the central-difference operator, $h = \Delta x$, and $k = \Delta t$. The equations above are precisely of this form. The method used to converge to a solution at each time step, is to iterate according to an under-relaxed Gauss-Seidel scheme. See Mitler (1988) for more details.

F. Improvements in CIGARET Over CIG25

There are five categories of improvements in CIGARET:

- The physics has been improved.
- The input is much more user-friendly. It also accepts input from SUBSTRAT.
- The output is in a form which can be used directly by SUBSTRAT.
- The program has been redesigned to be quasi-interactive with SUBSTRAT and can calculate the effects a substrate has on the smoldering.
- The documentation is improved.

These are described in the next three subsections. There is one more improvement which does not fit into any of the above five categories: The power of personal computers has increased substantially in the past six years, so that it is now feasible to run the program on a 486-level computer. Therefore the

program has been modified to run on a PC, rather than on a CYBER, as was the case for the antecedent program, CIG25.

1. Physics

The improvements in physics are four:

1. The gas density is now given by the ideal gas law, rather than taking it to be constant in the oxygen and the gas velocity equations, as was done earlier. See equations (97) and (103). In CIG25 the approximation was made that the product $\rho_g D_e$ could be taken from inside the derivatives in the first two terms on the right-hand side of equation (103). This eliminated the effects of gradients in the equations, and also allowed ρ_g to be factored out from all terms in that equation but the last. That is, in the identity

$$\frac{1}{\rho_g}\nabla\cdot(\rho_g D\nabla y) = D\nabla^2 y + T\nabla y\cdot\nabla\left(\frac{D(T)}{T}\right) \tag{130}$$

the second term on the right-hand side (where the ideal gas law was used to eliminate ρ_g), was dropped. This term has now been inserted into the program. Note that here we have taken into account not only the gradients in the gas density, but those of the diffusion coefficient as well.

2. Likewise, the char density now behaves correctly in the velocity subroutine, rather than assuming ρ_c also to be constant. In equation (97), the reaction rate R_{CO} depends on the char density (which falls with time). In CIG25, the density was taken to be constant, in this equation. Similarly, so was the gas density, ρ_g. Both of those densities now vary with time and position, properly.

3. The view factors for radiation exchanges have been calculated (see Section IV) and incorporated into CIGARET.

4. The radiation losses from the surface of the cigarette are now correctly calculated. That is, they are as given by equations (114), (116), and (148), rather than using the linearized form

$$\phi_{loss} \approx h'(T_c - T_a) \tag{131}$$

where h' is an effective heat transfer coefficient, which only approximates the effect of radiation loss.

2. Input and Output

The input section has been redesigned for much greater ease of comprehension and use. For example, the program now requests dimensional physical quantities, rather than the ratios used in the program and called for in the input section of CIG25. The program has also been redesigned so that it can indirectly interact with SUBSTRAT. See the USERS' GUIDE (Section II.H), for further discussion of these points.

The output files have been changed to accomplish the following:

- There is a complete "dump" at the end of each output time (file CIGOUT2), *the previous dump being eliminated.* This permits one to resume a calculation which has been interrupted for whatever reason. It also keeps the file from being too large.

- A small subset of CIGOUT2, the axial and the surface temperature distributions, is saved at each time step, and added to the other output file, CIGOUT1. SUBSTRAT uses only the surface distribution part.

It is appropriate at this point to indicate the modifications which have been made to TMPSUB2 to produce SUBSTRAT:

- SUBSTRAT uses the cigarette surface temperature distribution computed by CIGARET and passed to SUBSTRAT via the file CIGOUT1, to create the incident flux distribution. TMPSUB2 created a prescribed flux distribution used by the program, using a simple formula whose coefficients were obtained from its input file (magnitude of peak flux, σ_x, σ_y, prescribed velocity v). See equation (G2), Appendix G.

- SUBSTRAT now produces the file CIGIN1, to be used by CIGARET.

- What was previously called "initial x-position of (the flux) peak" (on the substrate) is now the x = 0 end of the cigarette.

3. Documentation

Besides the present report, the internal documentation in CIGARET has been somewhat expanded over what was in CIG25, so as to make it easier to follow the program. Also, the NOMENCLATURE section includes many of the symbols used in the program, which again facilitates understanding it, for anyone who wishes to do so.

G. RESULTS

1. Sensitivity of Calculation

The temperature dependence of the reaction rate given by equations (108) and (110) is very strong. Thus, assume the peaked spatial dependence

$$T(x) \approx T_a + \Delta T \exp\left[-(x - x_o)^2/\sigma^2\right] \tag{132}$$

for T, where $\Delta T \equiv T_{max} - T_a$. (See equations (C9) and (F2)). Then it is not difficult to show that the width of the resulting reaction rate distribution is approximately $\sigma\sqrt{\delta}$, where

$$\delta \equiv \frac{T_m}{T_m - T_a} \frac{T_m}{T_A + T_m}, \tag{133}$$

$T_m = T_{max}$, and $T_A \equiv E_A/R$ is the activation temperature. T_A is of the order $T_A \sim 22{,}000$ K, while $T_m \approx 1000$ K. Hence $\delta << 1$, and the reaction rate distribution R(x) is quite narrow. Hence the gradient is high:

$$\frac{\partial R}{\partial x} \approx \frac{0.63 R_m}{\sigma\sqrt{\delta}}, \tag{134}$$

where R_m is the peak reaction rate. Integration of the reaction over a volume shows that we must also have

$$R_m \sim \frac{const}{\sigma^2 \delta}. \tag{135}$$

Hence

$$\frac{\partial R}{\partial x} \propto (\sigma\sqrt{\delta})^{-3}, \tag{136}$$

and the gradient thus rises rapidly with T_A. Thus the grid size must be adequately small in order for the numerics to adequately cope with this. In fact, with a grid size $\Delta x = 0.2$ mm, the program could not converge with $T_A = 22{,}660$ K, the measured value. The "brute force" approach would be to halve the grid size to 100 microns. Not only would that quadruple the computational time to impractical levels, it could not even be done with DOS-based PC's, because of inadequate memory space. It was therefore necessary to use a lower, "model" value for T_A. To compensate, we also lowered the pre-exponential factor such that the rate constant was approximatly correct in the temperature range of interest. The program converges with $T_A = 15{,}000$ K.

2. Velocity of Smolder Wave

Three 30-second runs were made with the input data shown in the sample input data, Section III.H.4, to obtain 90 seconds of free smolder by this hypothetical cigarette. Some of the results are shown in Figure 22. The upper and lower curves in that figure show the positions of the intersections of the 600 K isotherms with the surface, as a function of time. Note that these isotherms enclose the reaction zone. Since the distance between them is still growing at t = 90 s, it is clear that a steady state has not yet been reached.

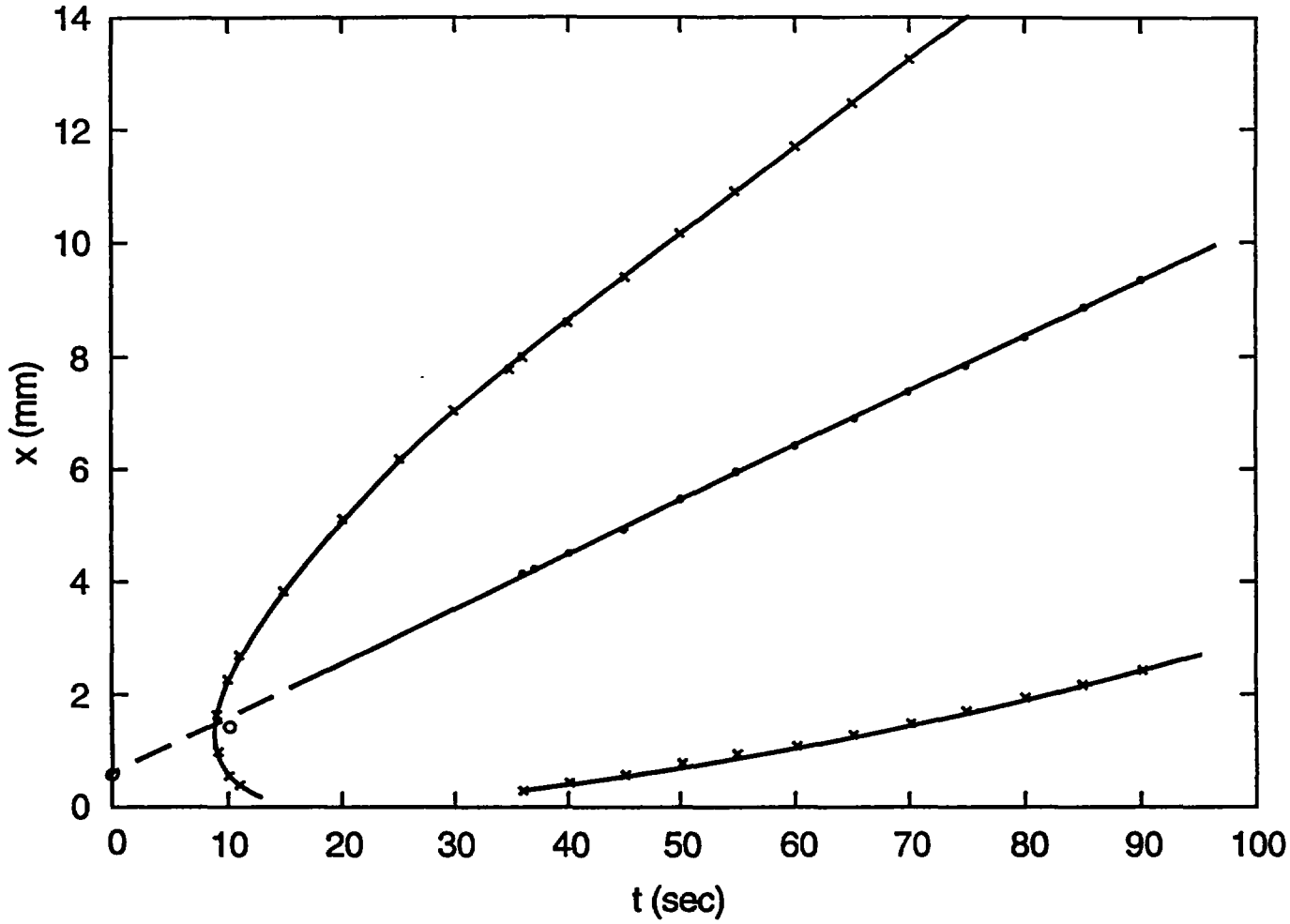

Figure 22. Result of a sample run with CIGARET. The upper and lower curves show the positions of the intersections of the 600 K isotherms with the surface, as a function of time. The central line is the locus of the midpoints between the curves.

Assuming that the isotherms are approximately symmetrical fore-and-aft, we have taken the midpoints of the intersections of the 600 K isotherms at the surface to represent x_0, "the" position of the smolder wave front. The fore-and-aft symmetry is not, in fact, perfect: the same procedure used for several different isotherms at t = 60 s yields the values shown in Table 6.

Table 6. Position of Cigarette Smolder Front at 60 Seconds as a Function of the Choice of Isotherm

Isotherm (K)	x_0 (mm)
600	6.4
700	6.6
800	6.7

Thus, as can be seen, although the "centroid" positions depend on which isotherm is chosen, the differences are quite small, so that the 600 K isotherm is representative of the front.

The central curve shown in the figure is the mean value of the isotherms, which we may refer to as $\langle x \rangle_{600}$. The points have been joined by a straight line, in fact, indicating that the smolder wave (regression) velocity calculated this way is remarkably constant in the period shown, even though a steady state has not (yet) been achieved. The slope of this line is V_{600} = 5.36 mm/min, a reasonable velocity.

The peak temperature in this calculation is not always on the axis. Although it is not plotted, the position of the peak temperature is <u>not</u> a good indicator of the regression rate during these first 90 seconds. At times it does not make any forward progress at all, for example. As the smolder continues, steady state would presumably be approached; when that eventually happens, of course the peak temperature will then move at the same velocity.

3. Temperature Profiles

The temperature profiles at t = 60 s, from the run described above, are shown in Figure 23 as a function of x, the distance from the cigarette tip. The upper curve is that on the axis; the lower one, the surface temperature. Note that the axial temperature peak is at x = 3.2 mm, well forward of the surface peak, at x = 5 mm. The interior peak evidently corresponds to the cone tip, and therefore it is quite reasonable that the peak should be in front of the surface peak. Note, further, that the paper burn line must be at 450 °C = 723 K, and that that occurs at x = 10.8 mm; hence the cone length is 10.8 - 3.2 = 7.6 mm, a not unreasonable length.

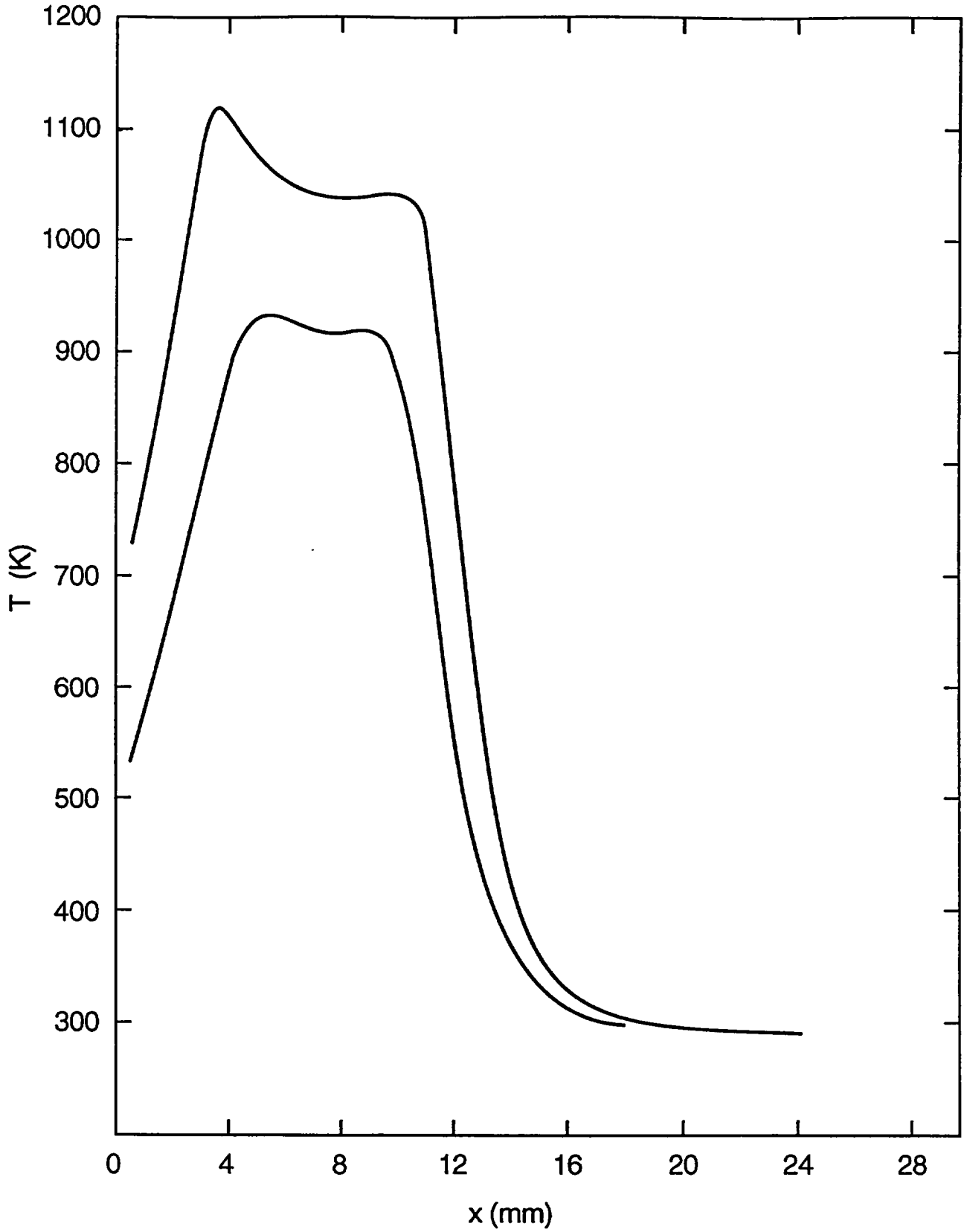

Figure 23. Longitudinal temperature distributions, along the axis and along the surface, at t = 60 s, for a sample run with CIGARET.

H. USERS' GUIDE

1. Running CIGARET

CIGARET and two helper programs together with the SUBSTRAT program are available on a diskette for IBM PC-compatible computers. The distribution diskette includes both executable and source code for CIGARET and SUBSTRAT, executable code for the helper programs, and sample input files. The CIGDATA program is used to prepare data files for CIGARET. CIGDATA must be run on an IBM PC-compatible computer with VGA graphics. CIGARET requires a 486 class PC (no graphics needed) in order to achieve satisfactory performance. On a 486/33 computer, 1 second of simulation time requires about 6 minutes of clock time, a factor of over 300, for $\Delta x = 0.2$ mm (3172 nodes). Running the program on a Silicon Graphics workstation, which is about 20 times faster than a 486/33 computer, is much more satisfactory.

The CIGARET source code (file CIGARET.FOR) can be compiled using any ANSI FORTRAN compiler. All CIGARET input and output files are ASCII files. Therefore, CIGARET can be recompiled and run on a different computer, while still using CIGDATA and SUBSTRAT on a PC and transferring files between the computers. A different computer may allow CIGARET to execute faster.

The user should be sure to inspect the README file on the distribution diskette. One way to read this file is to place the diskette in drive A: (or drive B:) and type

MORE <A:README or **MORE <B:README**

A permanent copy may be made with

PRINT <A:README

The README file contains a list of all files on the diskette, instructions for installing the necessary files on your hard disk, and information on any changes or additions to the program.

There should be at least 1 MB available on your hard disk. It is best to create a single subdirectory for the executable programs and related data files. This will allow you to easily delete all the files related to this program when you are finished with it. In general, *keep all files in the current working directory.*

Install the CIGARET program following the instructions in the README file. For example, from the directory on the hard disk where you want CIGARET installed and with the diskette in A:, type

A:INSTALL A:

2. Input and Output Files

All input for CIGARET must be placed in a data file, whose contents are described in Section III.H.4. This file is read as the "standard input stream," so CIGARET executes on MS-DOS and UNIX computers by redirecting the input file. For example, begin a run by typing

CIGARET < CIG1.DAT

where "CIG1.DAT" is the name of your input data file. [There is a sample input file available on the distribution diskette, TEST2.DAT]. As CIGARET completes each time step during the simulation, it displays the time (in seconds), the iteration number (K) within the current time step, and the time step number (IT). This allows you to monitor the progress of the simulation. At first, it takes over 100 iterations per time step to converge; as time goes on, fewer and fewer iterations are required, until as few as two or three suffice.

Two files are written by CIGARET:

CIGOUT1 provides cigarette surface temperature data for the SUBSTRAT program which are used to determine the incident heat flux on the substrate.

CIGOUT2 contains a dump of the cigarette field variables, which allows the program to be restarted at any future time (see Section III.H.3).

3. Restarting a Run

CIGARET can be aborted in the usual way by pressing CTRL and C at the same time. The dump file CIGOUT2 will be produced.

A terminated run (either aborted or terminated in some other way) can be restarted by using the dump file CIGOUT2. First, change its name to CIGIN2. Then, the input file (CIG1.DAT, in our example) must be edited by changing the last data value in the file from 0 to 1; this alerts the program to use CIGIN2 to initialize the variables. Then type "CIGARET < CIG1.DAT" as before, and the execution begins.

If a run is expected to be prohibitively long, it can be run in several steps. However, since a new copy of CIGOUT1 is produced every time CIGARET is run, it is necessary to save and then merge these files into a single CIGOUT1 file. This is best done by renaming each file as it is created. For example, type

RENAME CIGOUT1 CIGOUT.1,

RENAME CIGOUT1 CIGOUT.2, etc.

Finally, combine the files by using the CMERGE program:

CMERGE CIGOUT.1 CIGOUT.2 ... CIGOUT.N

The above command merges the specified files to create a new CIGOUT1.

4. Contents of the Data File

Line	Variables		Brief description
1	NR NZ RAD	NR	number of cells in radial direction
		NZ	number of cells in axial direction
		RAD	radius of cigarette [cm] (normalization: R)
2	PH PH1 DP	PH	void fraction
		PH1	total void fraction
		DP	diameter of pores [cm]
3	D1 D2 D3	D1	tobacco density / gas density
		D2	char density / tobacco density
		AN	ash density / tobacco density
4	SPHGS A FK	SPHGS	Cp(air) / Cp(tobacco)
		A	1/[density(solid)*Cp(sol)*R^2] [cmK/J]
		FK	thermal conductivity of tobacco [W/cmK]
5	D CN GK	D	oxygen diffusion coefficient / R^2 [s^{-1}]
		CN	mass of oxygen / mass of char consumed
		GK	thermal conductivity of gas [W/cmK]
6	B C E	B	pre-exponential factor * density [1/s]
		C	heat of combustion / Cp(tobacco)
		E	activation temperature [K]
7	TA TP EC	TA	ambient/initial temperature [K]
		TP	paper ignition temperature [K]
		EC	cigarette surface emissivity, ε_A
8	YA GAR GARP	YA	ambient oxygen mass fraction
		GAR	mass transfer coefficient for air,/R: γ_g/R [1/s]
		GARP	combined coefficient (air+paper): $R^{-1}(\gamma_p^{-1} + \gamma_g^{-1})^{-1}$
9	ISP INP IEB	ISP	number of time steps
		INP	number of time steps between data outputs
		IEB	number of time steps between energy balance checks
10	TS1 TS2 ERR	TS1	time step for first 50 steps [s]
		TS2	time step for later iterations [s]
		ERR	Gauss-Seidel convergence criterion
11	IDATA	IDATA	1 = read CIGIN2 to restart CIGARET

Sample Data File
(Note: the number of spaces between inputs on a line is arbitrary.)

```
21  151  0.40
0.65  0.85  0.0575
627.  0.341  0.13
0.777  6.5  3.16E-3
0.7  1.6428  4.514E-4
1.1085E9  13461.5  1.50E4
293.15  723.15  0.73
0.232  8.225  2.725
10000  200  80000
0.005  0.005  0.001
0
```

5. Producing a Data File

The CIGARET input data file can be created with any ASCII line editor. CIGDATA creates these data files interactively and thus uses certain commands which restrict its operation to IBM PC-compatible computers. It includes some checking of the input data. CIGDATA is especially useful for creating a data file which is only slightly different from another data file. This is useful in performing the parametric studies for which CIGARET was designed.

There are two special files in CIGARET to help the user with CIGDATA:

> The help file, CIGDATA.HLP, contains the text of the interactive help messages. Help is activated by pressing the F1 function key. If the help file is not available in the current working directory, no interactive help will be available.
>
> The configuration file, CIGDATA.CFG, sets the colors of the display. The file included on the distribution diskette assumes that a standard VGA monitor is being used. If the configuration file is not in the current working directory, a set of default colors will be used. A new configuration file can be made by using the MAKECFGT program. See the README file for instructions.

The operation of CIGDATA is explained on the following pages, which show the messages and input screens which will appear as the program is run. After reading through these pages, try using CIGDATA with one of the sample data files. Begin the program by typing **CIGDATA**. Abort the program by pressing CTRL and C simultaneously.

Data input screens from CIGDATA:

Screen 1: (primary menu)

```
==========================================================
CIGARET data preparation:

   #   File information

   #   Geometry data

   #   Tobacco data

   #   Pyrolysis data

   #   Gas data

   #   Boundary data

   #   Simulation control

   #   Exit data preparation

Use cursor keys to move between menu selections.
Press ENTER to activate the menu selection at the X.
Press ESC to return from a selection.  Press F1 for help.
```

Screen 2:

```
==========================================================

File data:                          press ESC when done;  press F1 for help.

    Name of old data file: ▓▓▓▓▓▓▓▓▓▓

    Name of new data file: ▓▓▓▓▓▓▓▓▓▓
```

Screen 3:

```
==========================================================

Geometry data:                      press ESC when done;  press F1 for help.

          Radius of cigarette: ▓▓▓▓▓▓▓▓▓▓ [mm]

 Number of cells in radial direction: ▓▓▓▓

  Number of cells in axial direction: ▓▓▓▓
```

Screen 4:

```
Tobacco data:                          press ESC when done;  press F1 for help.
        Density of tobacco: [          ] [kg/m^3]
     Thermal conductivity: [          ] [W/m K]
            Specific heat: [          ] [kJ/kg K]
             Void fraction: [          ]
       Total void fraction: [          ]
          Diameter of pores: [          ] [mm]
```

Screen 5:

```
Reaction data:                         press ESC when done;  press F1 for help.
   Pre-exponential factor: [          ] [m^3/kg s]
   Activation temperature: [          ] [K]
          Heat of reaction: [          ] [kJ/kg]
  Oxygen mass / char mass: [          ]
           Density of char: [          ] [kg/m^3]
            Density of ash: [          ] [kg/m^3]
```

See the explanatory note on the next page re "Activation temperature."

Screen 6:

```
Gas data:                              press ESC when done;  press F1 for help.
  Thermal conductivity of the gas: [          ] [W/m K]
          Specific heat of the gas: [          ] [kJ/kg K]
      Oxygen diffusion coefficient: [          ] [m^2/s]
```

Screen 7:

```
Boundary data:                          press ESC when done;  press F1 for help.
     Initial/ambient temperature: [          ] [°C]
      Paper ignition temperature: [          ] [°C]
            Cigarette emissivity: [          ]
    Ambient oxygen mass fraction: [          ]
Mass transfer coefficient through boundary layer: [          ] [m/s]
  Mass transfer coefficient through virgin paper: [          ] [m/s]
```

Screen 8:

```
Simulation control:                     press ESC when done;  press F1 for help.
             Total number of time steps: [          ]
          Steps between outputs to substrate: [     ]
           Time step for first 50 steps: [          ]
         Time step for later iterations: [          ]
      Gauss-Seidel convergence criterion: [          ]

    ( ) begin simulation with default start-up conditions
    ( ) read CIGIN2 to resume a simulation
```

Activation Temperature: As in TMPSUB2 (and therefore in SUBSTRAT), we use the activation temperature of the reaction, defined as:

$$T_A \equiv E_A/R$$

(where E_A is the activation energy and R is the universal gas constant), as the input parameter, rather than E_A itself.

I. SUMMARY OF SECTION III

The dynamics of a freely smoldering cigarette have been discussed. Similarly, what happens when it is resting on a substrate has been considered. Some of the mathematical models designed to simulate a smoldering cigarette have been outlined. Then the equations that must be satisfied by a cylindrically symmetric, homogeneous model of a cigarette quietly (freely) smoldering in air have been set down, within some specified simplifying assumptions (Section III.D.1). The effects of the paper wrapping, which pyrolyses away, are included.

The present program, CIGARET, is the outgrowth of an earlier model, CIG25, which employed some simplifications to the equation; principally, the neglect of pyrolysis (which has relatively little consequence in terms of the energy balance). CIGARET is a much-improved program in a number of ways which are described in detail in Section III.F. The numerical method used for solving the equations is described, and some of the problems discussed, in Section III.E. A primer on the use of CIGARET is given in Section III.H.

Some of the results obtained from using CIGARET are given in Section III.G. One remarkable result is that after ignition, the velocity of the resulting smolder wave quickly becomes constant, long before a steady state is achieved. The region in which char oxidation is proceeding rapidly (the glowing region) is correctly calculated to be conoid-shaped, and of the correct length.

IV. SIMULATING A BURNING CIGARETTE ON AN IGNITABLE SUBSTRATE

A. Introduction

The process which we are simulating is the heating and possible ignition of a substrate by a cigarette. In order to do that, the models SUBSTRAT and CIGARET developed in Sections II and III must be used in conjuction with each other. In this Section, the effects which take place when the lit cigarette and the substrate are in intimate contact are discussed. Next, it is shown in Section IV.C how the two programs are to be used in tandem in order to simulate the interaction. Finally, the effects are then calculated in detail. It is not essential that the reader read these last subsections in order to be able to use the program intelligently.

B. Qualitative Description

Consider the effects of a cigarette on a horizontal substrate that might affect the ignition of the substrate:

- The principal effect is the heating of the substrate by the hot cigarette coal.
- If any oxidative reaction takes place in the substrate, the cigarette competes with the substrate for oxygen.
- Some of the water vapor and tar emitted by the cigarette may recondense on the surface of the substrate and change its thermal characteristics.
- The cigarette affects the boundary conditions on the substrate: it interferes with convective cooling over the entire length of the cigarette.

Conversely, the horizontal substrate will influence how the cigarette smolders and thereby affect the likelihood that the cigarette will ignite it:

- The cold substrate initially provides a substantial conductive heat sink to the cigarette.
- If the substrate eventually undergoes exothermic reactions, it will heat the cigarette, instead.
- The substrate obstructs access of oxygen to the cigarette.
- If the substrate begins to react with oxygen, then the oxygen depletion for the cigarette would become still more severe.

These effects fall into two categories: gas transport effects and thermal effects. Consider the former first. There is a boundary layer surrounding the cigarette, within which the oxygen concentration drops as the surface is approached. Oxygen is supplied to the combustion site by the ambient *via* diffusion, as indicated by the arrows in Figure 23. The proximity of the substrate reduces the availability of oxygen to the cigarette from below. This will tend to inhibit the smoldering rate. This effect can be simulated by assuming that $y_a < 0.232$; CIGARET is given the information through the input file. See Section IV.D.4.

Thermally, the colder substrate cools the cigarette near the line of contact with the substrate, further inhibiting smoldering. This sink is not constant: as time progresses, the substrate heats up, and its cooling effect becomes progressively weaker. Radiative losses from the cigarette are decreased both because the cigarette is cooler and because one of the "targets" for this heat is warming and re-radiating back to the cigarette. If the heat loss from the cigarette is sufficiently high, the cigarette goes out. This effect is schematically indicated as curve A in Figure 21. If the substrate is not inert and exothermic reactions take place, cooling may be replaced by heating; this is sketched as curve B in the figure. This effect is also given in the input file for the cigarette, through the surface boundary conditions, as discussed in Section IV.D.

When both the cigarette and the substrate are reacting with oxygen, they are concurrently (a) generating heat, which accelerates their heat production, and (b) competing for oxygen, which retards their heat production. The modeling of effect (a) has been extensively described in Sections II and III; the modeling of (b) is not treated in this study.

C. Use of the Two Programs

It is important to understand how CIGARET and SUBSTRAT are used to obtain the interaction between the smoldering cigarette and the substrate with which it is in contact. The cigarette-substrate interaction is obtained through the boundary conditions which apply to each of the two models.

A full simulation requires an iterative use of CIGARET with SUBSTRAT (Section IV). Before starting, one should be sure there is no file named CIGIN1. First, run CIGARET (see Section III.H), generating CIGOUT1. The latter is now read by SUBSTRAT by typing

SUBSTRAT < INPUTFILE

(see Appendix B). [This was done before for TMPSUB2, as well.]

SUBSTRAT now produces a new input file, CIGIN1, for the CIGARET program. This file contains substrate surface temperature data which become part of the boundary conditions for the cigarette. Then run CIGARET, which will read CIGIN1 and create a new CIGOUT1. This simulation now includes an estimate of the influence of the substrate on the cigarette. Then run SUBSTRAT again, and so forth until convergence is obtained. *The input data files produced by the user for CIGARET and for SUBSTRAT (as distinct from the files produced by the programs themselves) must remain the same during these iterations.*

Since the principal effect of the cigarette is to heat the substrate, how to find the heat flux from the cigarette to the substrate will now be considered in detail. Then, the reciprocal effects of the substrate on the cigarette are discussed.

D. DETAILED CALCULATIONS OF INTERACTIONS

1. Conduction Flux to Substrate

We begin by calculating the heating flux delivered to the substrate by the cigarette. The substrate starts out at the ambient temperature and is in fair thermal contact with the cigarette. As shown in Figure 24, the measured flux is the initial (and momentary) flux from the cigarette to the cold substrate at the very small area of contact between them, along the LC (line of contact). The peak measured flux shown is about 5.6 W/cm^2. Since the measured coal surface temperature there was about 550 °C, the (net) blackbody radiation to the ambient is 2.56 W/cm^2. Muramatsu measured $\varepsilon_A = 0.73$; hence the actual radiation loss (assuming a grey body) is $\phi_{rad} = 1.9$ W/cm^2. This leaves 5.6 - 1.9 $\approx$ 3.7 W/cm^2 loss rate via conduction. With a surface temperature of 550 °C and an ambient temperature of 20 or 25 °C, one infers that the effective heat transfer coefficient is 71 W/m^{2}K, about seven times what it is in air. This large flux (5.6 W/cm^2) heats the substrate rapidly, so that the net flux, given by the first part of equation (137), falls rapidly to lower values.

The flux distribution $\phi(x)$ shown in Figure 24 is that along a narrow region (1.5 mm wide) about the line of contact; that is, it is $\phi(x,0)$. In order to find the heating of the substrate, we must also know the transverse and time dependences of the flux: $\phi = \phi(x,y,t)$.

It has been assumed that the initial substrate surface temperature is the ambient temperature, *i.e.*, $T_s(x,0) = T_a$. The heating flux from the cigarette to the substrate along the CL, $\phi_c(x,0,t)$, is given by experiment, as in Figure 24; the flux from the (resulting) hot substrate, $\phi_s(x,t)$, is calculated by the substrate program.

Moving away from the line of contact, the temperatures rapidly approach ambient. Therefore, the convective heat transfer effects of the cigarette diminish and the heat transfer coefficient asymptotically falls to its ambient value. A reasonable approximation to how the net convective flux to the substrate must vary with y is

$$\begin{aligned}\phi_{net,c}(x,y) = {} & h_c[T_c(x) - T_s(x,y)]\Omega_c(y) \\ & + h_o[T_a - T_s(x,y)][1 - \Omega_c(y)]\end{aligned} \tag{137}$$

where h_c is the heat transfer coefficient for convective heat loss from the cigarette to the substrate at the point at the line of contact corresponding to the peak flux (about 71 W/m^{2}K). h_o is the heat transfer coefficient for convective heat loss from the surface to the ambient (about 10 W/m^{2}K), and $\Omega_c(y)$ is a fraction indicating the convective influence of the cigarette at the distance y. Note that the net convective flux "into" the surface can become negative. If the cigarette extinguishes, for example, the fluxes from the cigarette disappear, and $T_c - T_s$ is asymptotically replaced by $T_a - T_s$.

We can break this flux into two parts, one of which is independent of the substrate temperature, and the other of the cigarette temperature. Thus, the cigarette "emits" the convective flux

$$\phi_{cig,c} = h_c(T_c - T_a)\Omega_c \tag{138}$$

to the substrate at (x,y), and the substrate at that point loses energy (convectively) at the rate

$$\phi_{sub,c} = [h_o + (h_c - h_o)\Omega_c](T_s - T_a) \tag{139}$$

where the arguments x and y have been suppressed for the sake of brevity.

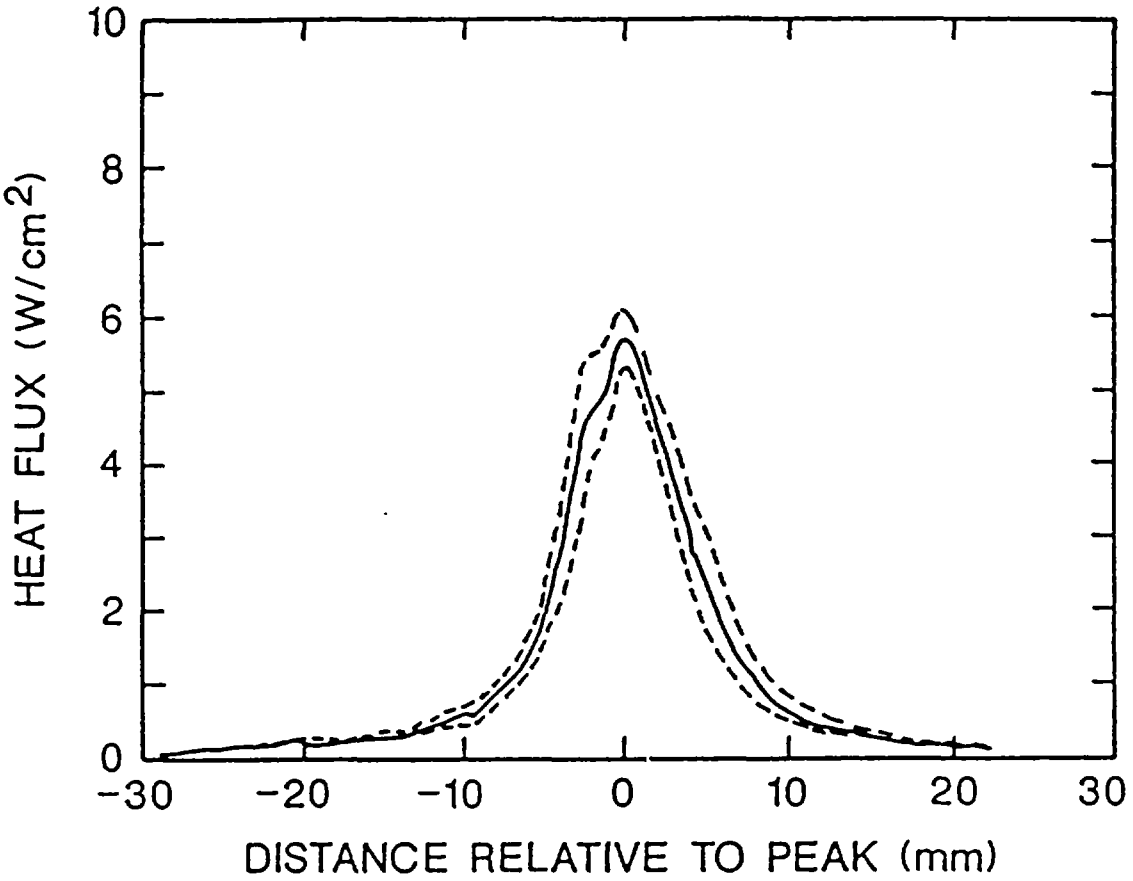

Figure 24. Flux emitted by a cigarette toward the substrate, along the contact line. The dashed curves indicate the probable errors (variance).

It is shown in Appendix G that $\Omega_c(y)$ can be approximated by a Gaussian. It follows that the effective heat transfer coefficient in equation (139) becomes

$$h_s(y) \approx h_o + \Delta h\, e^{-y^2/\sigma_y^2} \tag{140}$$

where

h_o = background $\approx$ 10 W/m^{2}K and $\Delta h = h_c - h_o \approx 61$ W/m^{2}K.

What is to be used for σ_y in equation (140) is discussed in Section IV.D.2, just below.

2. Radiative Flux to the Substrate

The radiation exchange experienced by the substrate at point (x,y) is

$$\phi_{net,r} = \epsilon_r \Omega \sigma (T_c^4 - T_s^4) - (1 - \Omega)\epsilon_s \sigma (T_s^4 - T_a^4), \tag{141}$$

where the x,y arguments have again been left out for clarity, and where

$$\epsilon_r \equiv \frac{\epsilon_c \epsilon_s}{1 - a} \tag{142}$$

is the effective emission coefficient. The radiation flux is treated in the same way as the convective flux; that is, this is split into an effective radiation flux from cigarette to substrate,

$$\phi_{cig,r} = \epsilon_r \Omega \sigma \left(T_c^4 - T_a^4\right), \tag{143}$$

while the substrate radiates away at the rate

$$\phi_{sub,r} = \left[\epsilon_r \Omega + \epsilon_s (1 - \Omega)\right] \sigma \left(T_s^4 - T_a^4\right) \tag{144}$$

In Appendix 5-D of Gann *et al.* (1988), it was shown that the variance of the Gaussian approximation to the convective distribution is about 0.57R. In Appendix H of the current work, it is found that Ω is reasonably well-approximated by a Gaussian also, of variance s. In Appendix G, it is shown that the joint convective-plus-radiative flux distribution is also approximated by a single Gaussian. We therefore use the approximation

$$\Omega_c(y) \approx \Omega(y) \approx \exp\left(-y^2/\sigma_y^2\right) \tag{145}$$

(See equation (H13)). Since we found above that $\sigma_y \approx 3.2$ mm for R = 4mm, we may assume, in general, that the net variance is 0.8R:

$$\sigma_y = 0.8R \tag{146}$$

(Also see equation (H14)).

3. Complete Flux

The cigarette, substrate, and net fluxes are the sums of the convective and radiative contributions. Adding together the terms from the two previous subsections, we can, for the general case, write this in the form

$$\phi_{net} = \phi_{cig} - \phi_{sub} \tag{147}$$

Here the flux at (x,y) from the cigarette is

$$\phi_{cig}(x,y) = h_c \Omega_c (T_c - T_a) + \epsilon_r \Omega \sigma \left(T_c^4 - T_a^4\right) \tag{148}$$

while the loss from the substrate to the ambient surroundings at (x,y) is

$$\phi_{sub}(x,y) = h_s (T_s - T_a) + [\epsilon_r \Omega + \epsilon_s (1 - \Omega)] \sigma \left(T_s^4 - T_a^4\right) \tag{149}$$

where the x-dependencies of T_c and T_s are not shown explicitly in the terms on the right, for the sake of brevity. These model fluxes hold for $0 \leq x \leq L$. ϕ_{cig} is the model flux from the cigarette; ϕ_{sub} is the model flux loss from the substrate.

We note that this separation does not quite succeed in giving a flux ϕ_{cig} which depends only on cigarette/air properties and another which depends only on substrate/air properties. However, ϕ_{cig} does not depend (as it must not) on $T_s(x,y,t)$, and ϕ_{sub} does not depend on $T_c(x,y,t)$. The separation into ϕ_{cig} and ϕ_{sub} is thus good enough that one can run the CIGARET and SUBSTRAT programs independently. One obtains the effects of the cigarette on the substrate from using, as input to SUBSTRAT, the flux ϕ_{cig} which is independent of T_s. On the other hand, by using ϕ_{sub}, one gets the surface losses of the substrate without having to know $T_c(x)$. Of course the substrate "knows" about the cigarette through the latter's flux, ϕ_{cig}, which is entered as an input to CIGARET. The substrate temperature equally influences the cigarette, but by a slightly different mode; that is discussed in the next Section.

4. Effects of the Substrate on the Cigarette

We next consider the inverse problem. The energy losses of the cigarette will be affected by the presence of the surface. Those effects are estimated in this Section. Moreover, since CIGARET is a model of a *freely* smoldering cigarette, the only way we can determine the effect of the substrate on it is to express the cigarette loss rate so that it appears to be simply losing energy to the air. This can be done by using an effective heat transfer coefficient and an effective surface emissivity, such that the presence of the substrate is correctly, if "covertly," taken into account. This is in fact possible to do, as is shown below.

Thermal Effects: Convection. It is shown in Appendix F that the convective loss of the cigarette can be expressed as:

$$\phi_{c,con} = h^* (T_c - T_a), \tag{150}$$

where

$$h^* \approx 21.22 - 10.47\left(\frac{T_s - T_a}{T_c - T_a}\right) - 9.02\left(\frac{T_c - T_{c,min}}{T_c - T_a}\right) \qquad \text{W/m}^2\text{K} \qquad \text{(F10)}$$

In deriving this, it was assumed that there is no longitudinal dependence of temperature for either the cigarette or the surface. We now relax this assumption, and recognize that there are longitudinal variations for both T_c and T_s. To be consistent with the approach outlined below equation (H11), we assume equation (F10) to be valid at every x, independent of adjacent regions. That immediately gives the x-dependence of h* to some approximation. This will likely be a weak dependence. Consider the middle term in equation (F10). Along a constant-y line (*e.g.*, $y = y_o$), the smaller $T_c(x)$ is, the smaller will be $T_s(x,y_o)$, since that substrate surface temperature was produced by T_c. That suggests that the ratio $(T_s - T_a)/(T_c - T_a)$ in equation (F10) will not vary strongly with x.

In order to use equation (F10), we must know $T_{c,min}$. This temperature is defined in Appendix F; it is the lowest temperature around the cigarette circumference, and lies at the contact line. This varies with time, as well as with x; hence $h^* = h^*(x,t)$. Also τ, as defined by equation (F8), is a function of t. The resulting $T_{c,min}(t)$ is found in Appendix I. The result is that the temperature difference between the top and the bottom of the cigarette is δT_{max}, given by

$$\delta T_{max} \approx 0.62\, r\, \bar{T} \qquad \text{(I5)}$$

where

$$\bar{T} = \frac{T_a + T_c}{1 + r} \qquad \text{(I1)}$$

and where r is the ratio of the thermal inertias of the materials:

$$r \equiv \sqrt{\frac{(k\rho c)_s}{(k\rho c)_c}} \qquad \text{(I2)}$$

We assume that this minimum temperature is reached in two seconds. It is indicated in Appendices F and I that this is the drop at the flux peak. The drop will be smaller away from the peak, and we may expect something like

$$\delta T_{max}(x,t) \approx \delta T_{max}(x_o,t)\left[\frac{T_c(x,t) - T_a}{T_c(x_o,t) - T_a}\right] \qquad \text{(151)}$$

to hold.

It has been observed that it takes quite a long time for the cigarette to "recuperate" from this drop in (lower) surface temperature, assuming it does not, in fact, extinguish. Again for the sake of simplicity, we will take the recovery period to be 2 minutes.

Suppose the cigarette is dropped onto the substrate at time t_o. Then collecting all these observations, we obtain the estimate

$$\tau(x,t) = \begin{cases} \delta T_{max}(x,t)\,(t-t_o)/2 & t_o \le t \le t_o+2 \\ \delta T_{max}(x,t_o+2)\left(\dfrac{122+t_o-t}{120}\right) & t_o+2 < t < t_o+122 \\ 0 & t > t_o+122 \end{cases} \tag{152}$$

where

$$\tau(x,t) \equiv T_c(\theta=\pi/2,x,t) - T_c(\theta=0,x,t) \tag{F8}$$

With these specifications, equation (F10) can be implemented.

Thermal Effects: Radiation. We next determine how the **radiation losses** of the cigarette are modified by the presence of the substrate. The radiation loss for the free cigarette at any point on its surface is given by equation (143), with ε_r replaced by ε_c. For the cigarette on the substrate, along the contact line, it is given by equation (H16). Notwithstanding the arguments made earlier about the difficulties in calculating the relevant radiation view factors, this was done, making some substantial simplifications.

We assume that the radiation flux emanating from the substrate is

$$\phi_s(y) \approx \phi_a + \Delta\phi \exp(-y^2/p^2) \tag{153}$$

where

$$\Delta\phi \equiv \epsilon_s \sigma T_s^4(y=0) - \phi_a \tag{154}$$

and

$$\phi_a \equiv \sigma T_a^4 \tag{155}$$

The x-dependence will be discussed in a moment. A certain fraction of that flux reaches the cigarette. Upon finding that fraction and integrating over y, it is found that the radiation loss of the cigarette, when in the presence of a substrate, is cut down from the usual expression to

$$\phi_{c,r} \approx \epsilon_c\left[\sigma T_c^4 - \frac{0.7}{\epsilon_s}\Delta\phi\right] - \epsilon_c\phi_a \tag{156}$$

where T_c is assumed to be independent of θ. (See Appendix F). The approximate factor 0.7 is the result of a large number of simplifications and numerical integrations. One of the assumptions is that $p = \sigma_y$.

In the $T_s(0) = T_a$ limit, equation (156) is approximately correct, since $\sigma T_c^4 >> \phi_a$, the deviation from exactitude is negligible. For higher temperatures $T_s(0)$, the flux ϕ_{cr} decreases, as it should, and is still a substantial fraction of σT_c^4 for the upper limit, $T_s(0) = T_c$.

Equation (156) can be written as

$$\phi_{c,r} \approx \epsilon_c^* \sigma T_c^4 - \epsilon_c \phi_a \tag{157}$$

where

$$\epsilon_c^* \equiv \epsilon_c \left[1 - \frac{0.7\,\Delta\phi}{\epsilon_s \sigma T_c^4} \right] \tag{158}$$

Finally, this must be generalized to include the dependence on x and t. Just as was done for the convective part, the simplest (although crude) way to do this is to generalize ε_c* by fiat to ε_c*(x,t), where

$$\epsilon_c^*(x,t) \equiv \epsilon_c \left[1 - \frac{0.7\,\Delta\phi(x,t)}{\epsilon_s \sigma T_c^4(x,t)} \right] \tag{159}$$

and

$$\Delta\phi(x,t) \equiv \epsilon_s \sigma T_s^4(x,0,t) - \phi_a \tag{160}$$

CIGARET can then be run without explicitly introducing the substrate temperature by using h*(x,t) and ε_c*(x,t) as the model heat transfer coefficient and cigarette emissivity. These are easily computed at each time step, in CIGARET.

In summary, explicit expressions for the transverse dependence of the cigarette and substrate fluxes have been found, which supplement the longitudinal dependencies. Thus, if the longitudinal dependence on the cigarette surface is known, the flux ϕ(x,y,t) can be found.

Fluid Flow Effects. Quite independently of any possible "competition" from the substrate for oxygen (that is, for oxidative reactions), access to air is somewhat restricted from below because of the presence of the substrate. Thus, the effect of having the substrate there is equivalent to limiting the indrawn-oxygen rate to what it would be in the open, but with $y_a < 0.23$. This effect is incorporated in running CIGARET through the appropriate value for y_a being supplied by the user in the input file.

In order to see what a small reduction in y_a produces, CIGARET was run with the same input parameters as yielded the results shown in Figures 22 and 23, but one: y_a was taken as 0.21. The result, however, was that the simulated cigarette extinguished after a few seconds. [The criterion used to declare the cigarette "extinguished" is that the peak surface temperature falls below 700 K (427 °C)]. Yet, when the cigarette surface temperature history of the $y_a = 0.23$ run was translated into a flux, and the substrate described in Section II.E was exposed to this flux, the substrate ignited in 22 seconds. Clearly, these are contradictory results, and the effective value of y_a to be used for this cigarette lying on this substrate should be between 0.21 and 0.232. It will probably not be very different for other cigarette/substrate combinations.

V. ACKNOWLEDGEMENTS

The authors wish to thank Dr. Thomas J. Ohlemiller for the many insightful discussions on various aspects of the work, Dr. Richard G. Gann for his careful and helpful reading of the manuscript, and the Consumer Products Safety Commission for sponsoring this work.

VI. REFERENCES

Ames, W.F. (1969) *Numerical Methods for Partial Differential Equations*, Barnes and Noble, New York.

Baker, R. (1975) "Temperature Variation Within a Cigarette Combustion Coal During the Smoking Cycle," High Temperature Science 7, p.236.

Baker, R.R., and Crellin, R.A. (1977) "The Diffusion of Carbon Monoxide Out of Cigarettes," Beiträge zur Tabakforschung 9, No.3 (October), p.131.

Belytschko, T. (1983) "An Overview of Semidiscretization and Time Integration Procedures," Chapter 1 in *Computational Methods for Transient Analysis*, edited by T. Belytschko and T.J.R. Hughes, North-Holland.

Bird, R.B., Stewart, W.E., and Lightfoot, E.N. (1960) *Transport Phenomena*, Wiley, NY.

Brandrup, J., and Immergut, E.H., eds. (1990) *Polymer Handbook*, 3rd ed., Wiley, NY.

Carslaw, H.S., and Jaeger, J.C. (1959) *Conduction of Heat in Solids*, 2nd ed; Oxford University Press.

Childs, G.E., Ericks, L.J., and Powell, R.L. (1973) "Thermal Conductivity of Solids at Room Temperature and Below," NBS Monograph 131, National Bureau of Standards, Gaithersburg, MD.

Clausing, A.M. (1969) "Numerical Methods in Heat Transfer" in *Advanced Heat Transfer*, Ed. B.T. Chao, University of Illinois Press, Urbana, IL.

Cohen, N. (1961) "Boundary-Layer Similar Solutions and Correlation Equations for a Laminar Heat Transfer Distribution in Equilibrium Air and Velocities up to 41,000 Feet per Second," NASA Technical Report R-118.

Conte, S.D. and de Boor, C. (1972) *Elementary Numerical Analysis*, McGraw-Hill, NY.

Croft, D.R., and Lilley, D.G. (1977) *Heat Transfer Calculations Using Finite Difference Equations*, Applied Science Publishers Ltd., London.

Egerton, A., Gugan, K., and Weinberg, F.J. (1963) "The Mechanism of Smoldering in Cigarettes," *Combustion and Flame* 7, p.63.

Gann, R.G., Harris, R.H. Jr, Krasny, J.F., Levine, R.S., Mitler, H.E., and Ohlemiller, T.J. (1988) "The Effect of Cigarette Characteristics on the Ignition of Soft Furnishings," NBS Technical Note 1241, National Bureau of Standards, Gaithersburg, MD.

Gugan, K. (1966) "Natural Smoulder in Cigarettes," *Combustion and Flame* 10, p.161.

Hilsenrath, J., Beckett, C.W., Benedict, W.S., Fano, L., Hoge, H.J., Masi, J.F., Nuttall, R.L., Touloukian, Y.S., and Woolley, H.W. (1955) *Tables of Thermal Properties of Gases*, NBS Circular 564, National Bureau of Standards, Gaithersburg, MD.

Holman, J.P. (1981) *Heat Transfer* (5th ed.), McGraw-Hill, New York.

Kakaç, S., Shah, R., and Aung, W., eds. (1987) *Handbook of Single-Phase Convective Heat Transfer*, Wiley/Interscience, New York.

Kashiwagi, T., and Nambu, H. (1992) "Global Kinetic Constants for Thermal Oxidative Degradation of a Cellulosic Paper," *Combustion and Flame* **88** p.345.

Kunii, D. (1961) *Kagaku Kogaku* [Chem. Eng. (Japan)] **25** p.891.

Larkin, B.K. (1964) "Some Stable Explicit Difference Approximations to the Diffusion Equation," *Mathematics of Computation* **18** p.196.

Lawson, J.R. (1993) National Institute of Standards and Technology, unpublished data.

Lendvay, A.T., and Laszlo, T.S. (1974) "Cigarette Peak Coal Temperature Measurements," *Beiträge zur Tabakforschung* **7**, p.63.

Miller, A.L. (1991) "Where There's Smoking There's Fire," *NFPA Journal*, p.86.

Mitler, H.E., and Davis, W.D. (1987) "Computer Model of a Smoldering Cigarette," Annual Conference on Fire Research, National Bureau of Standards, Gaithersburg, MD, Nov. 1987.

Mitler, H.E., and Walton, G. (1992) "A Computer Model of the Smoldering Ignition of Furniture," NISTIR 4973, National Institute of Standards and Technology, Gaithersburg, MD.

Peyret, R., and Taylor, T.D. (1983), *Computational Methods for Fluid Flow*, Springer-Verlag, New York.

Moussa, N.A., Toong, T.Y., and Garris, C.A. (1977) "Mechanism of Smoldering of Cellulosic Materials," *Sixteenth Symposium (International) on Combustion*, The Combustion Institute, Pittsburgh, PA, p.1447.

Muramatsu, M., Umemura, S., and Okada, T. (1979) "A Mathematical Model of Evaporation-Pyrolysis Processes Inside a Naturally Smoldering Cigarette, *Combustion and Flame* **36**, p.245.

Muramatsu, M. (1981) "Study of Transport Phenomena Which Occur During Unforced Smoldering of Cigarettes," Res. Report No. 123 of the Japan Tobacco and Salt Monopoly (in Japanese).

Ohlemiller, T.J. (1985) "Modeling of Smoldering Combustion Propagation," *Progress in Energy and Combustion Science* **11**, p.277.

Ohlemiller, T.J. (1991) "Smoldering Combustion Propagation on Solid Wood," in *Fire Safety Science, Proceedings of the Third International Symposium* (Eds., G. Cox and B. Langford); Elsevier Publishing Co., London, p.565.

Ohlemiller, T.J. (1991) unpublished results.

Ohlemiller, T.J., Villa, K., Braun, E., Eberhardt, K.R., Harris Jr., R.H., Lawson, J.R., and Gann, R.G. (1993) "Test Methods for Quantifying the Propensity of Cigarettes to Ignite Soft Furnishings," Special Publication 851, National Institute of Standards and Technology, Gaithersburg, MD.

Özisik, M.N. (1980) *Heat Conduction*, Wiley-Interscience, New York, 1980.

Parker, W.J. (1985) "Prediction of the Heat Release Rate of Wood," *Fire Safety Science - Proceedings of the First International Symposium* (Eds., C.E. Grant and P.J. Pagni); Hemisphere Publishing Corp, p.207.

Parker, W.J. (1988) "Prediction of the Heat Release Rate of Wood," Ph.D. Thesis, George Washington University, Washington, DC.

Quintiere, J.G., Harkleroad, M.F., and Walton, W.D. (1983) "Measurement of Material Flame Spread Properties," *Combustion Science and Technology* **32** p.67.

Quintiere, J.G., and Harkleroad, M.F. (1985) "New Concepts for Measuring Flame Spread Properties," *Fire Safety Science and Engineering*, ASTM STP 882, T.Z. Harmathy, ed., ASTM, Philadelphia, PA, p.239.

Quintiere, J.G. (1988) "The Application of Flame Spread Theory to Predict Material Performance," *J. of Res. of Nat'l Bur. of Standards* **93**(1), p.61.

Raznjevic, K. (1976) *Handbook of Thermodynamic Tables and Charts*, Hemisphere Pub. Co., New York.

Samfield, M. (1986) private communication.

Sandusky, H.W. (1976) "A Computer-Simulated Cigarette Model for Use in the Development of Less Hazardous Cigarettes," Ph.D. Thesis, Princeton University, Princeton, NJ.

Schneider, P.J. (1973) "Conduction," *Handbook of Heat Transfer*, 1st Ed., Eds. W.M. Rohsenow, & J.P. Hartnett, McGraw-Hill, New York.

Siegel, R., and Howell, J.R. (1981) *Thermal Radiation Heat Transfer*, 2nd ed., McGraw-Hill, NY.

Sparrow, E.M., and Cess, R.D. (1978) *Radiation Heat Transfer*, McGraw-Hill, NY.

Summerfield, M., Ohlemiller, T.J., and Sandusky, H.W. (1978) "A Thermophysical Mathematical Model of Steady-Draw Smoking and Predictions of Overall Cigarette Behavior," *Combustion and Flame* **33**, p.263.

Szekely, J., Evans, J., and Sohn, H. (1976) *Gas-Solid Reactions*, Academic Press, New York.

Thomas, P.H. (1957) "Some Conduction Problems in the Heating of Small Areas on Large Solids," *Quart Journ. Mech. and Applied Math.*, Vol. X, Pt. 4.

Torrance, K.E. (1985) "Numerical Methods in Heat Transfer," *Handbook of Heat Transfer Fundamentals*, 2nd Ed., Eds. W.M. Rohsenow, J.P. Hartnett, and E.N. Gacic, McGraw-Hill, New York.

Touloukian, Y.S., Powell, R.W., Ho, C.Y., and Klemens, P.G. (1970) *Thermophysical Properties of Matter*, Vol.2, Thermal Conductivity, Nonmetallic Solids, IFI/Plenum.

Treybal, R.E. (1955) *Mass-Transfer Operations*, McGraw-Hill, New York.

Weast, R.C., Ed. (1976) *Handbook of Chemistry and Physics*, CRC Press, Cleveland, OH.

Wichmann, I.S. (1991) "On the Use of Operator-Splitting Methods for the Equations of Combustion," *Combustion and Flame* **83**, p.240.

APPENDIX A

CONDUCTION ALGORITHM TESTS

A computer program called TEMPSUB was developed as part of the earlier investigation into the ignition of furnishings by smoldering cigarettes (Gann *et al.*, 1988). This program modeled heat transfer in furniture, or in a "substrate," using a simple finite difference approximation (FDA) for a homogeneous substrate with uniform and constant properties. The research indicated that this program would have to be expanded to include a two-layer model (fabric + padding), pyrolysis of each layer, an asymmetric flux input, and a variable grid.

These features have been implemented in SUBSTRAT by using a slightly different approach to the FDA than was used in TEMPSUB. The original approach was to convert the differential equation for heat transfer into an FDA by a Taylor's series approximation. The new approach is based on the conservation of energy within a control volume. It is based on physical reasoning and is usually easy to apply. It is most useful for variable grids, convective boundary conditions, odd-shaped regions, etc. It is more difficult to obtain accuracy estimates for the control volume approach than for the Taylor's series approach. For simple cases involving uniform grids and homogeneous materials the two approaches lead to identical FDA's. See Torrance (1985) or Croft and Lilley (1977) for further details.

Since there is a considerable increase in the desired capabilities of the upgraded program, it was decided to develop a program which would allow extensive testing of the FDA. This program is called CTEST3 (Conduction TEST - 3 dimensional) which has the ability to model simple boundary conditions (constant temperature, heat flux, or convection coefficient) on any of the six faces of the region.

The FDA used in CTEST3, the explicit Euler method, has been checked against several heat transfer problems which have analytic solutions. The first few tests involve various combinations of constant temperature, heat flux, and convection coefficient boundary conditions with analytic solutions from the classic text by Carslaw and Jaeger (1959).

Several of these analytic solutions involve the error function which is defined by

$$\mathrm{erf}(x) = \frac{2}{\sqrt{\pi}} \int_0^x e^{-\xi^2} d\xi \tag{A1}$$

so that $\mathrm{erf}(0) = 0$,

$\mathrm{erf}(\infty) = 1$,

and $\mathrm{erf}(-x) = -\mathrm{erf}(x)$.

The complementary error function is also used. It is defined as

$$\mathrm{erfc}(x) = 1 - \mathrm{erf}(x) = \frac{2}{\sqrt{\pi}} \int_x^\infty e^{-\xi^2} d\xi \tag{A2}$$

so that $\mathrm{erfc}(0) = 1$,

and $\mathrm{erfc}(\infty) = 0$.

Repeated integrals of the error function are also useful in conduction problems. These are defined by the recursive relationships

$$i^n\mathrm{erfc}(x) = \int_x^\infty i^{n-1}\mathrm{erfc}(x)\,dx \qquad n=1,2,... \tag{A3}$$

or

$$i^0\mathrm{erfc}(x) \equiv \mathrm{erfc}(x) \tag{A3a}$$

$$\mathrm{ierfc}(x) \equiv i^1\mathrm{erfc}(x) = \frac{e^{-x^2}}{\sqrt{\pi}} - x\,\mathrm{erfc}(x) \tag{A3b}$$

$$2ni^n\mathrm{erfc}(x) = i^{n-2}\mathrm{erfc}(x) - 2x\,i^{n-1}\mathrm{erfc}(x) \qquad n=2,3,... \tag{A3c}$$

See Appendix II of Carslaw and Jaeger (1959) for further details on error functions. Computer subroutines were written implementing these functions for the computation of the analytic solutions of the heat transfer tests.

Test 1: One-Dimensional Steady-State Conduction

CTEST3 has been tested for steady-state conduction with constant thermal properties and uniform grid spacing. This test sets opposite faces on a cubic region to different temperatures and makes the remaining faces adiabatic. After a sufficient number of time steps the temperature within the region should vary linearly from the hot to the cold face:

$$T(x) = T(0) + \frac{x}{L}[T(L) - T(0)] \tag{A4}$$

This has been confirmed in all three directions.

Test 2: One-Dimensional Transient Conduction, Constant Heat Flux Boundary Condition

This test was used in the development of the original substrate model. The analytic case for a constant flux involves a homogeneous solid occupying the semi-infinite region $x > 0$. The solid is initially at zero temperature throughout. At time $t = 0$, a constant heat flux, q, is applied to the $x = 0$ surface. The temperature within the region is given by Carslaw and Jaeger (1959), p. 75, equation (6):

$$T(x,t) = \frac{q\sqrt{4\alpha t}}{\kappa}\,\mathrm{ierfc}\left(\frac{x}{\sqrt{4\alpha t}}\right) \tag{A5}$$

Preliminary testing (again using a uniform grid and constant thermal properties) indicated that as Δt and Δx decreased, there was a uniform approach to the analytic solution. As for the accuracy to be expected, for $\Delta x = 1$ mm and $\Delta t = 0.5$ s, the error (after the first three time steps) was < 1 percent. We note that the results of test did not agree with results from the original TEMPSUB model. Further investigation indicated an error in the TEMPSUB boundary conditions subroutine. Correcting this error brought results from the two programs into complete agreement.

Tests show that reducing the grid size along with corresponding reduction of the time step cause the FDA solution to approach the analytic solution. Therefore, the FDA is consistent. Reducing the time step without changing the grid size does not improve the accuracy of the solution. In fact, it is best to operate as close to the stability limit as possible for both accuracy and execution time. Use of the variable grid gives results consistent with the uniform grid at the surface. The error in the calculated surface temperature goes down as time increases.

Test 3: One-Dimensional Transient Conduction, Constant Convection Coefficient Boundary Condition

This test represents a slab of a homogeneous solid of thickness 2L in the x direction and infinite extent in the y and z directions which is initially at unit temperature throughout. At time t = 0 the temperature of the fluid on both sides of the slab is changed to zero and heat is convected from the slab through a constant convection coefficient. Because of symmetry this problem is equivalent to a slab of thickness L with one adiabatic surface at x = 0 and a convective surface at x = L. The temperature within the region is given by Carslaw and Jaeger (1959), p. 122, equation (12):

$$T(x,t) = \sum_{n=1}^{\infty} \frac{2B\cos(\delta_n x/L)}{[B^2+B+\delta_n^2]\cos\delta_n} e^{-\delta_n^2 F} \qquad \text{(A6)}$$

where $B = hL/\kappa$ (Biot number),
$F = \alpha t/L^2$ (Fourier number), and
δ_n are the solutions of the transcendental equation $\delta_n \tan\delta_n = B$.

In order to check the calculation of this complicated analytic solution, the solution to a related problem was also computed. This is the temperature in a semi-infinite slab with the convective boundary condition (Carslaw and Jaeger (1959), p. 72, equation (5)):

$$T(x,t) = \text{erfc}\left(\frac{x}{\sqrt{4\alpha t}}\right) - \exp\left(\frac{h}{\kappa}(x+\alpha h t/\kappa)\right)\text{erfc}\left(\frac{x}{\sqrt{4\alpha t}} + \frac{h}{\kappa}\sqrt{\alpha t}\right) \qquad \text{(A7)}$$

where x is now the distance from the convective surface into the region. There is good agreement between the FDA and analytic solutions. Again, the error in the calculated temperature goes down as time increases.

Test 4: Three-Dimensional Transient Conduction, Constant Surface Temperature Boundary Condition

This test represents a block of a homogeneous solid in the region defined by -a < x < a, -b < y < b, and -c < z < c which is initially at unit temperature throughout. At time t = 0 the temperatures of the surfaces of the block are reduced to zero, and the block begins to cool. The temperature within the region is given by Carslaw and Jaeger (1959), p.184, equation (5):

$$T(x,y,z,t) = \frac{64}{\pi^3} \sum_{l=0}^{\infty} \sum_{m=0}^{\infty} \sum_{n=0}^{\infty} \frac{(-1)^{l+m+n}}{(2l+1)(2m+1)(2n+1)} \times$$
$$\cos\left[\frac{(2l+1)\pi x}{2a}\right] \cos\left[\frac{(2m+1)\pi y}{2b}\right] \cos\left[\frac{(2n+1)\pi z}{2c}\right] \times \tag{A8}$$
$$\exp\left\{-\frac{\kappa\pi^2 t}{4}\left[\frac{(2l+1)^2}{a^2} + \frac{(2m+1)^2}{b^2} + \frac{(2n+1)^2}{c^2}\right]\right\}$$

This expression requires the summation of many terms at small values of time, but only a few terms at large values of time. The implementation of this complicated equation had to be checked against simpler analytic cases. The first case represents a homogeneous solid occupying the semi-infinite region, $x > 0$. The solid is initially at unit temperature throughout. At time $t = 0$ the temperature at $x = 0$ is instantly reduced to zero. The temperature within the region is given by Carslaw and Jaeger (1959), p.59, equation (3):

$$T(x,t) = \text{erf}\left(\frac{x}{\sqrt{4\alpha t}}\right) \tag{A9}$$

The second case involves a solid which occupies the region $x > 0$, $y > 0$, $z > 0$. It is initially at unit temperature and at time $t = 0$ the temperature at the $x = 0$, $y = 0$, and $z = 0$ surfaces is instantly reduced to zero. The temperature within the region is given by Carslaw and Jaeger (1959), p. 184, equation (1):

$$T(x,y,z,t) = \text{erf}\left(\frac{x}{\sqrt{4\alpha t}}\right) \text{erf}\left(\frac{y}{\sqrt{4\alpha t}}\right) \text{erf}\left(\frac{z}{\sqrt{4\alpha t}}\right) \tag{A10}$$

The temperatures near the corners of the block should be very similar to this.

There was good agreement (error < 1%) for a test with a = 30 mm, b = 20 mm, c = 10 mm, and using a 1 mm uniform grid. The original variable grid model was found to be insufficiently accurate at points where the grid size changed. It was therefore replaced by the current uniformly increasing grid at a cost of some increase in code complexity; although the results are not quite as accurate as for the uniformly spaced grid, the difference is very minor.

Test 5: One-Dimensional Transient Conduction, Two Different Materials

This test consists of one material in the region 1 ($0 < z < L$) initially at unit temperature and another material in region 2 ($z > L$) initially at zero temperature. The boundary at $z = 0$ is adiabatic. At time $t = 0$ heat begins to be conducted between the two regions. The temperatures in the two regions are given by Özisik (1980), p. 328, equation (8-109):

$$T_1(x,t) = 1 - \frac{1-\delta}{2} \sum_{n=0}^{\infty} \delta^n \left\{ \operatorname{erfc}\left[\frac{(2n+1)L-x}{\sqrt{4\alpha_1 t}}\right] + \operatorname{erfc}\left[\frac{(2n+1)L+x}{\sqrt{4\alpha_1 t}}\right] \right\}$$

$$T_2(x,t) = \frac{1+\delta}{2} \sum_{n=0}^{\infty} \left\{ \operatorname{erfc}\left[\frac{2nL+\mu(x-L)}{\sqrt{4\alpha_1 t}}\right] - \operatorname{erfc}\left[\frac{(2n+2)L+\mu(x-l)}{\sqrt{4\alpha_1 t}}\right] \right\} \qquad \text{(A11)}$$

where

$$\mu = \sqrt{\frac{\alpha_1}{\alpha_2}}, \quad \beta = \frac{\kappa_1}{\kappa_2 \mu}, \quad \delta = \frac{\beta - 1}{\beta + 1} .$$

There was good agreement between the FDA and analytic solutions. It even worked well when the first layer was only one-half of a grid thick. This may be useful for thin fabric coverings.

Test 6: Three-Dimensional Transient Conduction, Constant Heat Flux Impinging on a Circular Area (Disk) on a Semi-Infinite Region.

The impinging flux is q, there is convective cooling from the surface, $h(T_s - T_a)$, and the disk radius is R. The temperature at the center of the heated area is given by Thomas (1957), equation (5):

$$T(t) = \frac{qR}{\kappa} \left\{ \sqrt{\frac{4\alpha t}{\pi R^2}} \left[1 - \exp\left(-\frac{R^2}{4\alpha t} \right) \right] + \operatorname{erfc}\left(\frac{R}{\sqrt{4\alpha t}} \right) \right\} -$$

$$- \frac{2q}{h} \int_{\omega=0}^{\frac{h}{\kappa}\sqrt{\alpha t}} \left[1 - \exp\left(\frac{-h^2 R^2}{4k^2 \omega^2} \right) \right] \omega e^{\omega^2} \operatorname{erfc}(\omega)\, d\omega \qquad \text{(A12)}$$

The first part of the above expression is the center point temperature if there is no convective cooling. Tests indicate that the accuracy of the FDA for this test is primarily dependent on how accurately the circular flux pattern is represented on the rectangular surface grid. A small grid and assigning cell heat gain according to the portion of the cell that is within the circle improve accuracy.

Note that tests 1 through 6 involve a step change, which should be the worst condition to simulate with the FDA. In all cases the maximum errors occurred at the first time step, and the error declined as time increased.

Test 7: Three-Dimensional Transient Conduction, Uniformly Moving Point-Source Heat Flux

This test consists of a point source of power Q moving in an infinite body at a constant velocity v in the x direction (Schneider (1973), pp.3-86, equation (78)):

$$\frac{\kappa r}{Q}(T - T_o) = \frac{1}{4\pi} \exp\left[-\frac{v}{2\alpha} (\xi + r) \right] \qquad \text{(A13)}$$

where $\xi = x - vt$ and $r = (\xi^2 + y^2 + z^2)^{1/2}$. Adjusting for a semi-infinite body with the point source moving along an adiabatic surface is done by replacing 4π by 2π in equation (A13). Generally good agreement was achieved for this test. Accuracy was limited by grid size near the point source and the fact the this is a quasi-steady case in that movement of the point source does not have a beginning point.

Larkin's Method

The FDA algorithm in CTEST3 was transferred directly into the new substrate model TMPSUB2. The addition of pyrolysis forced the use of a very small grid in the region of peak temperature for a satisfactory solution. This, combined with the stability requirement of the explicit Euler method, forced a very small time step and therefore a very long execution time. A different FDA algorithm had to be found to achieve a program fast enough to be useful. Larkin's method was chosen because of its simplicity in that it uses the same spatial FDA as the original method while the new temporal FDA does not require the solution of simultaneous equations.

CTEST3 was not rewritten to run all of the test cases, but several tests were made with TMPSUB2 (some using a modified surface boundary condition) which indicate the accuracy of the method for different grid size and time step options. The results of these tests are shown in Tables A-1, A-2, and A-3.

Table A-1 gives the results of several tests which can be compared to equation (A5) to determine the effect of grid spacing. These tests use a region 40 mm thick to simulate a semi-infinite body which is shown to be appropriate by having negligible heat flux at the constant temperature surface at Z=40 mm. Comparisons are made based on the temperature of the surface (Z=0 mm).

> Test 2a: Using a constant 1 mm grid spacing the temperature after 100 seconds is 0.33% less than the exact value.
>
> Test 2b: Using a constant 0.5 mm spacing gives a surface temperature 0.18% below the theoretical value.
>
> Tests 2c through 2f use variable grid spacing to reduce the number of cells and execution time at the cost of some loss of accuracy.

Table A-2 gives the results of several tests where the parameters that control the time step while maintaining a constant grid spacing, are varied. These parameters are the maximum time step, dtmax, and the maximum temperature change, dTmax. (Whenever $T_{n+1} - T_n$ exceeds dTmax, the time step is halved.) Obviously the greatest accuracy should be achieved with small values for these two parameters, but execution time is reduced by using large values. There is no obvious optimum; the user must choose values appropriate for results he wishes to achieve.

Table A-3 shows tests of different grid spacings for full three-dimensional heat conduction from a stationary spot heat flux. These tests use representative thermal properties for the fabric and padding. Various combinations of cell spacings are used to select the best grid.

Table A-1. Grid Spacing Tests

Thermal diffusivity: 2e-07 m^2/s Thermal conductivity: 0.1 W/mK
Surface heat flux: 1e+04 W/m^2 Distance from surface: 0 m

time	Texact	Test2a	Test2b	Test2c	Test2d	Test2e	Test2f
0.000	0.0000	0.000	0.000	0.000	0.000	0.000	0.000
0.125	17.8412	5.000	9.319	9.319	9.319	9.319	9.319
0.250	25.2313	9.643	16.889	16.889	16.889	16.889	16.889
0.375	30.9019	13.970	23.331	23.331	23.331	23.331	23.331
0.500	35.6825	18.298	28.916	28.916	28.916	28.916	28.916
0.625	39.8942	22.252	33.840	33.840	33.840	33.840	33.840
0.750	43.7019	26.206	38.035	38.035	38.035	38.034	38.034
0.875	47.2035	29.838	42.229	42.229	42.229	42.229	42.229
1.000	50.4627	33.469	45.757	45.757	45.757	45.757	45.757
1.250	56.4190	40.170	52.366	52.366	52.366	52.366	52.366
1.500	61.8039	46.383	58.208	58.208	58.208	58.208	58.208
1.750	66.7558	52.167	63.496	63.496	63.496	63.496	63.496
2.000	71.3650	57.577	68.361	68.361	68.361	68.361	68.361
2.250	75.6940	62.656	73.042	73.042	73.041	73.041	73.041
2.500	79.7885	67.445	77.173	77.173	77.173	77.173	77.171
2.750	83.6828	71.859	81.305	81.305	81.304	81.304	81.302
3.000	87.4039	76.273	85.049	85.049	85.048	85.047	85.044
3.500	94.4070	84.279	92.243	92.243	92.242	92.240	92.233
4.000	100.9253	91.625	98.911	98.909	98.908	98.904	98.893
4.500	107.0474	98.433	105.154	105.152	105.149	105.143	105.125
5.000	112.8379	104.796	111.046	111.042	111.038	111.030	111.002
6.000	123.6077	116.456	121.976	121.970	121.962	121.946	121.894
7.000	133.5116	127.018	132.004	131.993	131.981	132.050	131.966
8.000	142.7299	136.650	141.315	141.300	141.283	141.309	141.188
9.000	151.3880	145.711	150.034	150.014	149.991	149.993	149.830
10.000	159.5769	154.229	158.272	158.248	158.219	158.201	157.994
15.000	195.4410	191.150	194.315	194.266	194.208	194.109	193.654
20.000	225.6758	221.986	224.670	224.600	224.514	224.343	223.631
25.000	252.3132	249.025	251.396	251.307	251.195	250.960	249.998
30.000	276.3953	273.438	275.472	275.367	275.235	274.852	273.660
35.000	298.5410	295.758	297.599	297.487	297.339	296.828	295.425
40.000	319.1538	316.566	318.155	318.040	317.879	317.378	315.771
45.000	338.5137	336.042	337.525	337.408	337.234	336.650	334.844
50.000	356.8248	354.491	355.815	355.694	355.509	354.928	352.929
60.000	390.8820	388.738	389.887	389.758	389.550	388.899	386.532
70.000	422.2008	420.206	421.230	421.093	420.862	420.147	417.431
80.000	451.3517	449.479	450.409	450.262	450.010	449.235	446.188
90.000	478.7307	476.960	477.816	477.660	477.388	476.556	473.195
100.000	504.6265	502.943	503.740	503.574	503.282	502.397	498.738
cells:		41	81	35	25	18	12
steps:		153	154	154	154	153	153

TEST2A: dz=1.0mm, nz=41, nc=41, r=1.000, dtmax=1.0, dTmax = 5.0
TEST2B: dz=0.5mm, nz=81, nc=81, r=1.000, dtmax=1.0, dTmax = 5.0
TEST2C: dz=0.5mm, nz=35, nc=4, r=1.055, dtmax=1.0, dTmax = 5.0
TEST2D: dz=0.5mm, nz=25, nc=4, r=1.115, dtmax=1.0, dTmax = 5.0
TEST2E: dz=0.5mm, nz=18, nc=4, r=1.234, dtmax=1.0, dTmax = 5.0
TEST2F: dz=0.5mm, nz=12, nc=4, r=1.628, dtmax=1.0, dTmax = 5.0

Table A-2. Time Step Control Tests

Thermal diffusivity: 2e-07 m^2/s Thermal conductivity: 0.1 W/mK
Surface heat flux: 1e+04 W/m^2 Distance from surface: 0 m

time	Texact	Test2b	Test2g	Test2h	Test2J
0.000	0.0000	0.000	0.000	0.000	0.000
0.125	17.8412	9.319	9.093		
0.250	25.2313	16.889	16.685	20.000	20.000
0.375	30.9019	23.331	23.148		
0.500	35.6825	28.916	28.750	31.538	31.538
0.625	39.8942	33.840	33.688		
0.750	43.7019	38.035	38.107	39.690	39.690
0.875	47.2035	42.229	42.125		
1.000	50.4627	45.757	45.801	47.841	47.841
1.250	56.4190	52.366	52.390		
1.500	61.8039	58.208	58.223	58.553	58.553
1.750	66.7558	63.496	63.506		
2.000	71.3650	68.361	68.368	69.264	69.264
2.250	75.6940	73.042	72.899		
2.500	79.7885	77.173	77.158	77.403	77.403
2.750	83.6828	81.305	81.191		
3.000	87.4039	85.049	85.028	85.542	85.542
3.500	94.4070	92.243	92.222		
4.000	100.9253	98.911	98.891	97.831	97.831
4.500	107.0474	105.154	105.136		
5.000	112.8379	111.046	111.029	110.120	110.120
6.000	123.6077	121.976	121.963	120.390	120.390
7.000	133.5116	132.004	131.993	130.660	130.660
8.000	142.7299	141.315	141.312	139.622	139.622
9.000	151.3880	150.034	150.053	148.583	
10.000	159.5769	158.272	158.312	156.621	157.545
15.000	195.4410	194.315	194.402	192.945	
20.000	225.6758	224.670	224.773	223.337	221.615
25.000	252.3132	251.396	251.504	250.229	
30.000	276.3953	275.472	275.656	274.420	
35.000	298.5410	297.599	297.855	296.726	
40.000	319.1538	318.155	318.512	317.415	313.420
45.000	338.5137	337.525	337.900	336.887	
50.000	356.8248	355.815	356.236	355.255	
60.000	390.8820	389.887	390.336	389.440	382.464
70.000	422.2008	421.230	421.690	420.860	
80.000	451.3517	450.409	450.870	450.093	442.530
90.000	478.7307	477.816	478.274	477.541	
100.000	504.6265	503.740	504.191	503.495	495.723
cells:		81	81	81	81
steps:		154	724	106	42

TEST2B: dz=0.5mm, nz=81, nc=81, r=1.000, dtmax=1.0, dTmax = 5.0
TEST2G: dz=0.5mm, nz=81, nc=81, r=1.000, dtmax=1.0, dTmax = 1.0
TEST2H: dz=0.5mm, nz=81, nc=81, r=1.000, dtmax=1.0, dTmax = 20.0
TEST2I: dz=0.5mm, nz=81, nc=81, r=1.000, dtmax=4.0, dTmax = 5.0
(Same results as test2b because dT > 2.5 at dt = 1.0)
TEST2J: dz=0.5mm, nz=81, nc=81, r=1.000, dtmax=4.0, dTmax = 20.0

Table A-3. 3-D Transient Conduction Tests

time	test3a	test3b	test3c	test3d	test3e
0.00	0.000	0.000	0.000	0.000	0.000
1.00	65.749	70.904	71.046	71.254	71.301
2.00	88.450	91.190	91.381	91.660	91.723
3.00	104.807	106.828	107.053	107.382	107.455
4.00	118.536	120.437	120.692	121.060	121.140
5.00	130.745	132.693	132.974	133.375	133.460
10.00	178.269	180.414	180.785	181.287	181.377
15.00	211.444	213.792	214.214	214.765	214.850
20.00	236.140	238.668	239.121	239.692	239.766
30.00	269.762	272.068	272.539	273.119	273.173
40.00	291.304	293.512	293.988	294.550	294.585
50.00	305.937	308.182	308.659	309.201	309.219
60.00	316.279	318.588	319.064	319.589	319.594
70.00	323.830	326.195	326.670	327.180	327.176
80.00	329.498	331.903	332.376	332.876	332.865
90.00	333.853	336.285	336.757	337.248	337.233
100.00	337.271	339.718	340.188	340.673	340.654
cells:	18081	18081	18081	19176	18375
steps:	152	154	154	154	154
time:	303.08	316.37	316.10	338.90	346.32

TEST3A: dx=0.5mm, nx=41, ny=21, nz = 21, nc = 4, yw=zw = 40,
rx=ry=1.167, rz=1.187, dtmax=1.0, dTmax = 5.0

TEST3B: dx=0.25mm, nx=41, ny=21, nz = 21, nc = 4, yw=zw = 40,
rx=ry=1.240, rz=1.240, dtmax=1.0, dTmax = 5.0

TEST3C: dx=0.25mm, nx=41, ny=21, nz = 21, nc = 4, yw=zw = 30,
rx=ry=1.210, rz=1.210, dtmax=1.0, dTmax = 5.0

TEST3D: dx=0.25mm, nx=47, ny=24, nz = 17, nc = 4, yw=zw = 30,
rx=ry=1.161, rz=1.326, dtmax=1.0, dTmax = 5.0

TEST3E: dx=0.25mm, nx=49, ny=25, nz = 15, nc = 4, yw=zw = 30,
rx=ry=1.149, rz=1.431, dtmax=1.0, dTmax = 5.0